Resists for sub-20-nm electron beam lithography with a focus on HSQ: state of the art

2009 Nanotechnology 20 292001

(http://iopscience.iop.org/0957-4484/20/29/292001)

Nanotechnology **20** (2009) 292001 (31pp) doi:10.1088/0957-4484/20/29/292001

TOPICAL REVIEW

Resists for sub-20-nm electron beam lithography with a focus on HSQ: state of the art

A E Grigorescu and C W Hagen

Faculty of Applied Sciences, Delft University of Technology, Lorentzweg 1, 2628 CJ Delft, The Netherlands

Received 18 November 2008, in final form 13 February 2009
Published 1 July 2009
Online at stacks.iop.org/Nano/20/292001

Abstract

In the past decade, the feature size in ultra large-scale integration (ULSI) has been continuously decreasing, leading to nanostructure fabrication. Nowadays, various lithographic techniques ranging from conventional methods (e.g. photolithography, x-rays) to unconventional ones (e.g. nanoimprint lithography, self-assembled monolayers) are used to create small features. Among all these, resist-based electron beam lithography (EBL) seems to be the most suitable technique when nanostructures are desired. The achievement of sub-20-nm structures using EBL is a very sensitive process determined by various factors, starting with the choice of resist material and ending with the development process. After a short introduction to nanolithography, a framework for the nanofabrication process is presented. To obtain finer patterns, improvements of the material properties of the resist are very important. The present review gives an overview of the best resolution obtained with several types of both organic and inorganic resists. For each resist, the advantages and disadvantages are presented. Although very small features (2–5 nm) have been obtained with PMMA and inorganic metal halides, for the former resist the low etch resistance and instability of the pattern, and for the latter the delicate handling of the samples and the difficulties encountered in the spinning session, prevent the wider use of these e-beam resists in nanostructure fabrication. A relatively new e-beam resist, hydrogen silsesquioxane (HSQ), is very suitable when aiming for sub-20-nm resolution. The changes that this resist undergoes before, during and after electron beam exposure are discussed and the influence of various parameters (e.g. pre-baking, exposure dose, writing strategy, development process) on the resolution is presented. In general, high resolution can be obtained using ultrathin resist layers and when the exposure is performed at high acceleration voltages. Usually, one of the properties of the resist material is improved to the detriment of another. It has been demonstrated that aging, baking at low temperature, immediate exposure after spin coating, the use of a weak developer and development at a low temperature increase the sensitivity but decrease the contrast. The surface roughness is more pronounced at low exposure doses (high sensitivity) and high baking temperatures. A delay between exposure and development seems to increase both contrast and the sensitivity of samples which are stored in a vacuum after exposure, compared to those stored in air. Due to its relative novelty, the capabilities of HSQ have not been completely explored, hence there is still room for improvement.

Applications of this electron beam resist in lithographic techniques other than EBL are also discussed. Finally, conclusions and an outlook are presented.

(Some figures in this article are in colour only in the electronic version)

Contents

1. Introduction

1.1. Nanotechnology

A novel branch of technology, nanotechnology, arose in 1959 when Richard Feynman gave his famous (and now often-quoted) talk [1] at the annual meeting of the American Physical Society at the California Institute of Technology (Caltech) entitled 'There is plenty of room at the bottom: an invitation to enter a new field of physics'. With this visionary talk, Feynman anticipated a large spectrum of fields that are now well established such as electron and ion beam fabrication, nanoimprint lithography (NIL), quantum electronics, projection electron microscopy and microelectromechanical systems (MEMS). Although at that time the idea of making things smaller seemed a little unrealistic, Tom Newman [2] succeeded (in 1985) in writing the first page of Charles Dickens' novel *A tale of two cities* with a reduction factor of 25 000 using an electron beam lithography (EBL) machine. Each character of the written page was about 50 nm wide. Since then, an explosion of miniaturization has been observed, based on the development of micro- and nanotechnologies. Actually, nanotechnology has a long history and the first manufacturer of a nanostructure is nature itself because, for example, the width of a DNA molecule is about 2 nm. In 1905, Einstein [3] measured the size of a single sugar molecule and showed that each molecule is approximately 2 nm in diameter. Almost 30 years later, Knoll and Ruska [4, 5] made the imaging of nanometer structures possible, by developing the electron microscope. In 1932, Langmuir [6] discovered the existence of monolayers (layers with a thickness of one atom or one molecule). In 1968, Arthur and Cho [7] from Bell Laboratories developed a technique that can deposit single atom layers on a surface, namely molecular beam epitaxy. The word 'nanotechnology' was used for the first time in 1974 by Taniguchi [8] when he wanted to describe the technology which was operating in the nanometer range. In 1981, Binnig and Rohrer from IBM invented the scanning tunneling microscope [9], making it possible to image single atoms. In 1985 Kroto *et al* discovered fullerene [10], which measures about 1 nm in diameter. Five years later, Eigler *et al* from IBM [11] demonstrated that the position of the atoms can be precisely controlled. They wrote the name of their company on a nickel surface using 35 individual xenon atoms. Other milestones of nanotechnology are the discovery of carbon nanotubes by Iijima [12] and the fabrication of a transistor from a carbon nanotube by Tans *et al* [13] in 1998. In 2000, the first DNA motor was created by Lucent Technology and Oxford University [14]. These devices open up the possibility of making computers 1000 times faster than before. The idea is that the DNA motor can be attached to electrically conducting molecules to assemble rudimentary circuits which act as switches. The main goal of nanotechnology (which operates in the scale range of 1–100 nm) is to fabricate and use structures, devices and systems that have innovative properties and functions due to their small or intermediate size. In general there are two different approaches for nanostructure fabrication. The first one, called the 'top-down approach', includes different techniques (e.g. electron beam (e-beam) lithography, photolithography and NIL) which are focused on a progressive reduction of dimensions. The second approach, 'the bottom-up approach', uses techniques (e.g. molecular self-assembly, carbon nanotube synthesis) in which nanostructures are assembled out of smaller units, like atoms or molecules. The miniaturization process finds its application in a large variety of fields, such as microelectronics, biology [15], chemistry, optics and optoelectronics [16–18]. The continuous need of society for faster computers, high-density data storage [19] and high-speed information processing is the leading force behind nanofabrication in the industrial world.

1.2. Nanolithography

The main goal of lithography is to create a desired pattern in a resist layer and the subsequent transfer of that pattern into or onto the underlying substrate. The basic steps of a lithographic process are schematically illustrated in figure 1.

First, the substrate (often silicon) is cleaned using chemical baths or plasma procedures in order to remove contaminants which may lead to poor adhesion or defect formation in the resist layer. Sometimes, the surface of the substrate is modified by using an adhesion promoter, such as hexamethyldisilazane (HMDS), which enhances the adhesion of the resist to the substrate. In the next step, a resist layer (usually an organic polymer) is spin coated onto the substrate from a solution containing the resist dissolved in an appropriate casting solvent. Thinner resist layers can be obtained by using

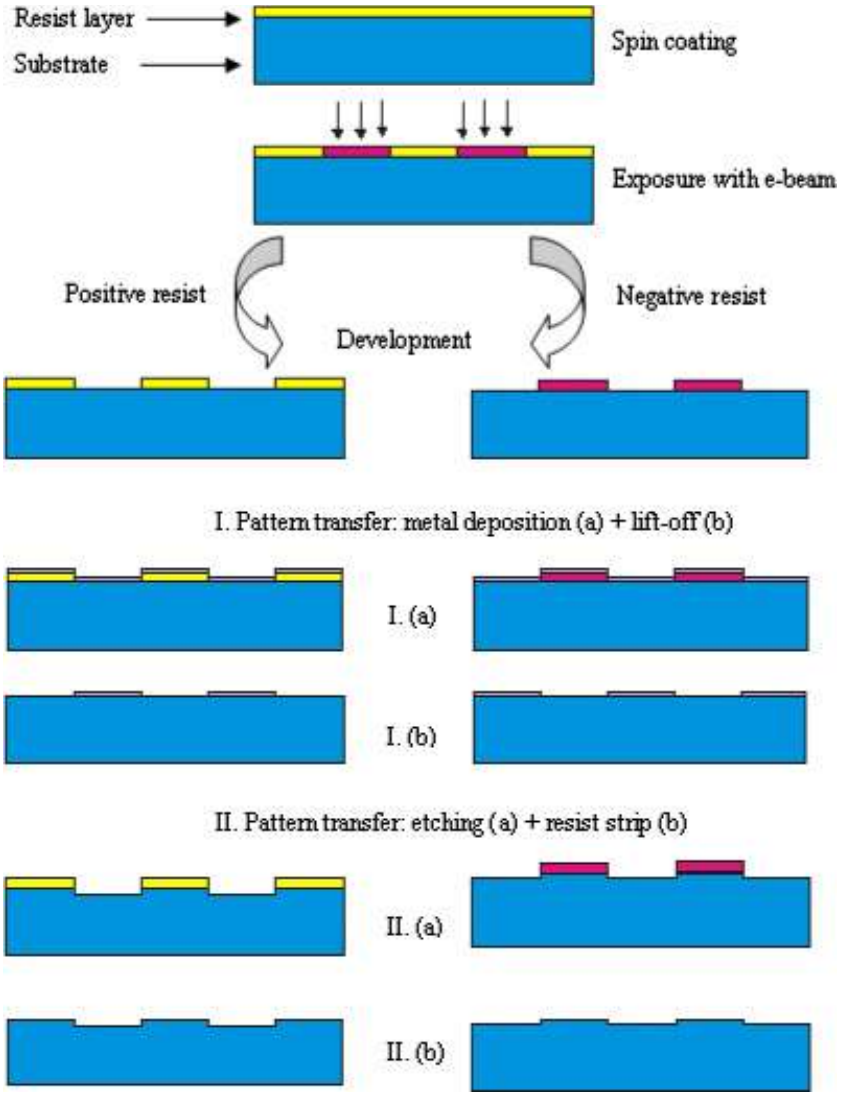

Figure 1. Schematic representation of the basic steps of a lithographic process including coating, exposure, development and pattern transfer such as lift-off or etching.

solutions with a higher dilution rate. After this, the sample is baked on a hotplate in order to remove the excess solvent from the resist and to thermally anneal residual stress in the resist built up during the spinning session. This step is referred to as a post-apply-bake (PAB). Next, assuming EBL, the sample is e-beam irradiated causing chemical changes in the exposed area which influence the solubility of the exposed area relative to the unexposed area of the resist in a developing solvent. Following e-beam exposure, the sample is baked again to either thermally anneal the exposed regions, in order to reduce unwanted chemical changes that might have been caused within the resist layer during the exposure, or to promote further chemical changes in the exposed or unexposed area. This step is referred to as a post-exposure-bake (PEB). Subsequently, the sample is developed through spray, puddle or immersion methods. A resist can have a negative or positive tone depending on whether the unexposed or the exposed regions are removed from the substrate during the development process. Usually, the patterns obtained are transferred into or onto the substrate by using techniques such as etching or lift-off. Finally, the resist structures are removed via a liquid stripping process or dry oxygen plasma etch without altering the properties of the layers beneath the resist. Lithography machines (exposure tools) and resists (imaging and recording media) play a crucial role in advanced nanolithography. Figure 2 [20] shows that in order to write very small structures in a very short time a lot of effort has to be made to improve both the lithographic tool and the resist process. The dashed line represents a phenomenological relationship between the resolution and throughput given by the following power law fit: resolution $\approx 2.3 A_t^{0.2}$, where resolution is measured in nanometers and the areal throughput (A_t) is in $\mu m^2\ h^{-1}$. Optical step and repeat reduction printing offers a high areal throughput at the expense of resolution. At the opposite extreme, manipulation of individual atoms at low temperatures using a scanning tunneling microscope (STM) ensures the finest resolution but has a very slow writing speed.

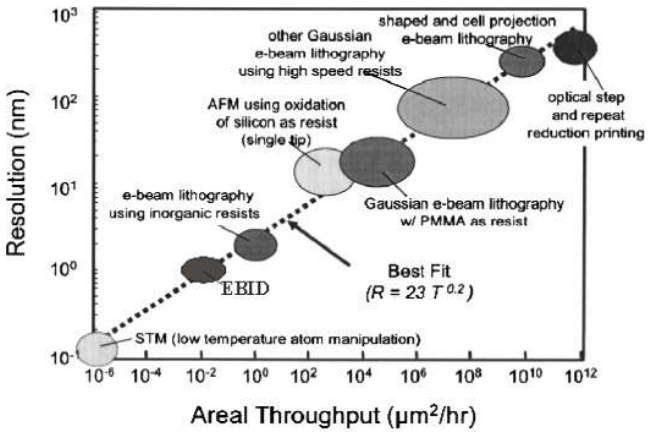

Figure 2. Resolution (nm) versus throughput (μm^2 h^{-1}) for different lithographic methods which have been demonstrated to date (adapted from [20] with the addition of results obtained by van Dorp *et al* [21] with e-beam induced deposition (EBID)). Adapted from [20].

1.3. Electron beam lithography

Electron beam lithography provides excellent resolution due to the small wavelength and a small probe size, whereas the resolution in optical lithography starts to become limited by the wavelength of the light that is used for exposure. In addition, EBL is a flexible patterning technique that can work with a variety of materials. The main drawback is that it is slow (typically 10^7 pixels s^{-1}) and too expensive for volume manufacturing. However, in the last decade, an impressive amount of work has been done to improve the performance of the EBL tool. The main characteristics an e-beam pattern generator should have are: a small spot size (down to a few nm), low cost (high throughput), high reliability (high yield) and the ability to write reproducible structures over large areas. There are two main e-beam writing strategies, projection printing and direct writing. In projection printing, a large e-beam pattern is projected parallel through a mask onto a resist coated substrate by using a high-precision lens system. In direct writing, a small e-beam spot is moved with respect to the wafer to expose the wafer one pixel at a time, eliminating the expensive and time-consuming production of masks. Typically the writing field, which is defined by the maximum deflection range of the e-beam, is of the order of a few hundred micrometers. Larger patterns require mechanical stage movements, which need to be very accurate in order to precisely stitch consecutive writing fields. Most exposures are performed with high-energy electrons (between 50 and 100 keV) because they provide very high resolution. The backscattered electrons from the substrate cause exposure of areas in the proximity of the intended pattern (proximity effect), which in most cases can be corrected for (proximity correction). In e-beam lithography at low energy (between 2 and 20 keV), the penetration depth of electrons is limited. In this case, electrons will lose (almost) all their energy in the resist layer, increasing the exposure efficiency (or the sensitivity) and the throughput of the lithography tool, but at the expense of a high resolution. Also, the proximity effect is reduced due to the minimization of the electron scattering effect from the substrate. There is no need to implement complicated computer algorithms to correct for the proximity effect, which is both expensive and time consuming. Still there are several disadvantages when using low acceleration voltages, for example an increase in the beam size, the requirement to use very thin resist layers or charging effects. If a thick resist layer is used, it is possible that electrons (which have a low penetration depth at low voltage) expose only a fraction of the resist thickness. During the development process, the unexposed underlying resist layer might be dissolved leading to a patterning failure.

For sub-100-nm resolution, the resist technology becomes an issue due to electron scattering, both in the resist and in the substrate. An ideal resist material should have high sensitivity, high contrast, high resolution, high plasma etching resistance for pattern transfer to the substrate and small molecular size. In order to reduce the volume of electron scattering, very thin resist layers should be used when high resolution is desired. A review of all the materials suitable for use as a high-resolution e-beam resist would be a titanic work, due to the impressive number of papers available in the literature. Because we are currently interested in sub-20-nm nanostructure fabrication, the goal of this review is to bring some order to the existing knowledge on various possible resists for this resolution range. In section 1.4, we describe the framework that should be considered when nanostructures are written. In section 2, an overview of existing high-resolution e-beam resists is given. In the following section, which is dedicated to hydrogen silsesquioxane (HSQ) e-beam resist, we present the properties which make the use of HSQ very attractive when sub-10-nm features are written using EBL. The changes that HSQ undergoes before, during and after e-beam exposure are presented step by step. Next, several applications of HSQ in other fields than EBL (e.g. extreme ultraviolet (EUV), NIL, step and flash imprint lithography) are discussed in section 4. The fifth and last section is devoted to conclusions and recommendations for future work.

1.4. Framework for the nanofabrication process

In the following paragraphs we will discuss the most important properties that the e-beam resist must have in order to become a suitable candidate for nanolithography.

Electron dose (usually expressed in μC cm^{-2}) is the number of electrons per unit area required to achieve the desired chemical response in the resist. Each lithographic process has an optimum dose which represents the dose at which the measured linewidth after development is equal to the designed linewidth. Exposing a pattern correctly usually requires the performance of a preliminary test exposure, referred to as a dose test. In this test, the same pattern is exposed at different doses and after the development process the optimum dose can be determined through inspection in a suitable inspection tool (scanning electron microscope, atomic force microscope, optical microscope, etc). The actual size of the patterned feature is drastically influenced by the electron dose. When a pattern is exposed at lower doses compared to the optimum dose (underexposure), the actual structure

width is smaller than the designed structure width but the probability for pattern irregularities also increases. The main consequence of overexposure (dose higher than the optimum dose) is a widening of the pattern size. In general, the electron dose should be low in order to achieve high sensitivity and throughput.

When exposing test patterns consisting of lines with different widths and pitches written with various exposure doses, the *line exposure dose* is another important parameter used to characterize the lithographic process. In order to obtain a very high resolution, the lines are written with a beam step size (the distance between two adjacent pixel exposures) that is as small as possible. Depending on the designed linewidth, an exposure is performed by scanning the beam once (single pass) over one (single exel or 1-exel) or n adjacent lines (n-exel line). The line dose is calculated by multiplying the area dose with the designed linewidth.

The process latitude (PL) represents the change in critical dimension (CD) for a given change in the exposure dose and it is given by the following expression:

$$\mathrm{PL}(\%) = 100(D_{[+10\%]} - D_{[-10\%]})/D_{[0\%]}$$

where $D_{[0\%]}$ represents the optimum dose and $D_{[\pm 10\%]}$ are the doses corresponding to a 10% increase or decrease in the feature size. Another definition for the PL (which is rarely used) is related to the development time:

$$\mathrm{PL}(\%) = 100(t_{[+10\%]} - t_{[-10\%]})/t_{[0\%]}.$$

Contrast and sensitivity are the most frequently used terms for the characterization of e-beam resist. In general, the e-beam resist is characterized by contrast curves, which can be easily obtained by plotting the remaining thickness after the development process versus the electron dose (figure 3). An ideal e-beam resist should have both a high contrast and a high sensitivity. Unfortunately, in reality, an increase in one of these parameters leads to a decrease in the other, and vice versa. A high sensitivity will provide a high throughput (e.g. reduction of the writing time), but in general leads to a shallower slope for the contrast curve, hence a lower contrast.

Contrast (γ), also called 'the vertical contrast', is defined as the slope of the linear portion of the falling edge (positive resist) of the remaining resist thickness versus log (dose) curve: $\gamma = \frac{1}{\log(\frac{D_2}{D_1})}$, where D_1 is the maximum dose at which still no film is lost (i.e. the linear portion of figure 3 extrapolated to 100%) and D_2 is the minimum dose at which all the resist thickness is lost (see figure 3). The sensitivity is defined as the dose for which all of the resist is removed (D_2 in figure 3). For thick resist layers and large structures, these curves are easy to obtain. In general, the remaining resist thickness after the development process is measured with a surface profilometer. When thin resist layers are used (<10 nm), reliable measurements are difficult to get, even when using an atomic force microscope (AFM) operating in tapping mode. In this case, the *'horizontal contrast'* is measured; this is defined as the slope of the linear portion of the graph of the linewidth measured after the development plotted versus the logarithm of the dose.

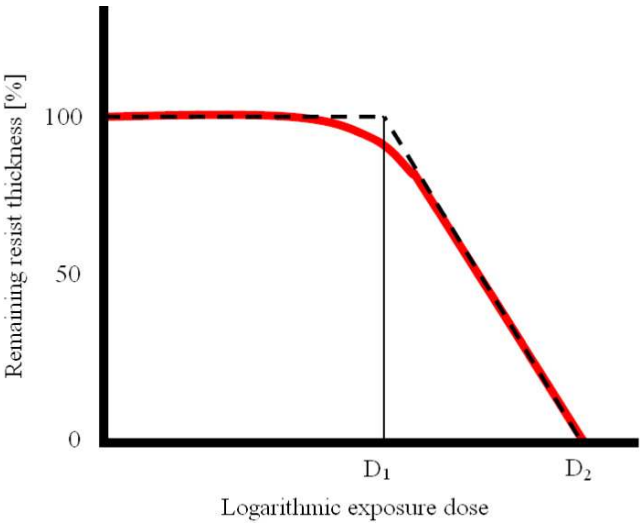

Figure 3. Remaining resist thickness versus dose for positive tone.

Line edge roughness (LER) or the linewidth fluctuation becomes a serious issue when the pattern size shrinks. For nanolithography, the LER should be as small as possible in order to avoid pattern distortion or deterioration of the resolution. The σ value (the root mean square (RMS) of the fluctuations in edge position) is the most frequently used parameter for characterization of LER. A typical measured value for LER is about 3 nm [22] or 10 nm (3σ) [23], when resists with a very high contrast are used. The LER is caused by various factors which range from the lithographic system (dose fluctuation, mask roughness) to resist materials and the development process. It becomes important to take shot noise effects into account. The statistics of electron arrival gives rise to dose variations, which translate to variations in the size of written structures. Nevertheless, the main cause for LER is represented by the polymer aggregates which are naturally present in all the resist layers. These polymer aggregates are built up of resist molecules and they can even reach 20–30 nm in size in commercial resists such as ZEP, SAL and PMMA. There are two ways to image these polymer aggregates: either by observing the cross section of the resist film using a scanning electron microscope (SEM), or by observing the resist surface after the development process using an atomic force microscope (AFM). The former metrological tool is most frequently used due to its simplicity and lower risk of damaging the sample. The presence of the polymer aggregates causes uneven dissolution rates between the aggregates and the surrounding areas, due to the density difference between these two regions. The surrounding areas of the aggregates, which have a lower density than the polymer aggregates, are quickly and completely dissolved. After that, the aggregated polymers are extracted from the surface, although it is possible that the dose is too low to achieve complete development. This phenomenon is known as 'aggregate extraction development'. A higher dose might limit the effect of the aggregates (to the detriment of resolution and high throughput) but it cannot completely eliminate the trapping of the aggregates at the edge of the pattern. At the edge of the pattern, aggregates

are not extracted and remain trapped in the sidewall after the development process. This is due to the low dose received by the sidewalls, impeding the dissolution of the areas which surround the aggregates. As a consequence, the shapes of the polymer aggregates appear at the edge of the pattern, causing LER. The LER is encountered in all e-beam resists and is more pronounced in lightly exposed regions. One way to overcome this limitation for nanolithography is to use resists with small molecular size which implies small aggregated polymers, e.g. HSQ or calixarene. Several authors have succeeded in improving the LER by reducing the differences between the dissolution rates in the polymer aggregates and surrounding areas. Yamaguchi *et al* [24] developed a novel type of resist by chemically amplifying the positive e-beam resist ZEP 520. After the baking procedure, the resist layer is cross-linked in such a way that there is no difference in density between the polymer aggregate and the surrounding areas. The LER was reduced to 2 nm in this novel e-beam resist, whereas the LER in a conventional ZEP resist is more than 3 nm, when isolated lines with a width of 100 nm are written.

The *resolution* (i.e. the capability of resolving very small features) of e-beam resists should also be high. Therefore, the resist should be very thin to minimize electron scattering, which is the resolution-limiting factor when very small structures are desired. In general, the patterned structures are lines and the repeating distance between adjacent features is called 'the pitch'. The lines can be classified into isolated (when the designed feature width is much smaller than the pitch) or lines and spaces (when the designed feature width is equal to half the pitch). When the pitch of the features decreases, achieving high resolution becomes a real challenge. The ultimate resolution test can never be performed on isolated features because it would be hard to tell whether the structures were under-exposed or over-developed, leading to a smaller linewidth. Therefore, lines and spaces should be written when the resolution is tested for a certain lithographic process.

Linewidth control and the reproducibility is the ability to maintain the same feature size across an entire sample and from one substrate to another, respectively, when the electron dose is kept constant. Linewidth control can be determined by measuring the size of the feature on different positions over a large area on one sample and then by plotting these values as a function of position. Furthermore, when this data are plotted as a function of time or batch number the reproducibility of the lithographic process can be visualized.

Etch resistance represents the ability of the resist to withstand an etching process and it is probably the most difficult requirement to achieve for a resist. After development, the pattern is usually transferred into the underlying resist layer or substrate by either a wet or dry etch process. Although wet etching offers high throughput and good selectivity (ratio of the etch rate of the film being etched to the etch rate of the underlying film or substrate), it can also cause a loss of adhesion of the resist, due to the interaction between the etchant solution and the resist itself. Moreover, wet etching is isotropic which means that the etching rate is equal in all directions. As a consequence, underetching will not only alter the size of the transferred pattern, but will also lose the vertical, anisotropic sidewalls. All these problems seem to be solved by using a dry etching process. In this case, a vertical profile is obtained, resulting in exact replication of the pattern in the underlying layer or substrate. The physical and chemical properties of the resist material represent the main limitations for the etching process. In general, a very high etch resistance is preferred.

Regarding the resist material, *the process window* is an important parameter when e-beam-based nanolithography is performed. It is well known that the resolution is limited by various factors such as baking temperature, resist material, delay time between baking and exposure, electron dose and the development process. The process window is just an indication of how much these factors can be varied without causing any appreciable loss in resolution or distortion of the pattern. If a resist has a wide process window for a certain factor mentioned above, that means that this factor might be varied but that it will not cause a major change in the resulting pattern.

An ideal resist material should have high sensitivity, high contrast, high resolution, high plasma etching resistance for pattern transfer to the substrate and small molecular size. In order to reduce the volume of electron scattering, very thin resist layers should be used when high resolution is desired.

2. High-resolution e-beam resists

Over the past decades, different types of resist materials have been investigated. In general, e-beam resists can be classified into two major categories: organic and inorganic. Electron beam resists are altered by the beam in such a way that, after development the portion exposed to the beam is removed (positive resist) or remains on the substrate after the unexposed portion is removed (negative resist). In general, resist materials are applied onto the surface of the substrate by spinning techniques and are dried to form a thin uniform layer of thickness depending on the application and the resolution (minimum feature size) required. In the following sections, we will discuss the properties of these e-beam resists and it should be stressed that we selected only published results on ultrahigh resolution especially in the sub-20-nm region, unless explicitly mentioned otherwise.

2.1. Organic resists

All e-beam resists consisting of carbohydrates are called organic resists and they are, typically, polymeric materials. Some of these resist polymers are discussed in the following paragraphs.

Since it was discovered [25], *polymethyl methacrylate* (PMMA) has been used as the standard resist for high-resolution e-beam lithography. During e-beam irradiation, the long polymer chains of PMMA are fragmented into smaller chains making it soluble in an appropriate solvent (usually methyl isobutyl ketone, MIBK). At the same time, a parallel process of polymerization occurs in which the polymer units are cross-linked together and form an insoluble material. At low exposure doses, the scission process dominates, allowing PMMA to be used as a positive tone e-beam resist. At high

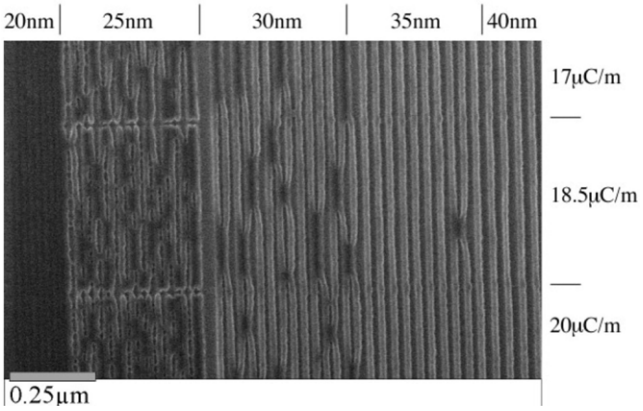

Figure 4. Dense lines written in a 40 nm PMMA negative tone resist layer. The exposure was performed at various pitches and doses as indicated in the figure [26]. Reprinted with permission from [26]. Copyright (1997), Institute of Physics.

exposure doses, the polymerization becomes more dominant and PMMA can also be used as a negative resist. In general, this negative tone is not often used due to the high exposure dose that is required to initiate it. Hoole *et al* [26] wrote lines approximately 15 nm wide at a 30 nm pitch in a 40 nm thick PMMA negative tone resist using an acceleration voltage of 300 keV and a 10 pA beam current. The line exposure doses (185 nC cm^{-1}) were almost 100 times higher than the ones usually used for positive tone PMMA. Acetone was used as the developer because it strips off very effectively the unexposed and partially exposed regions but is unable to remove the polymerized PMMA from the exposed area. In a similar experiment, the pattern was successfully transferred into a Au/Cr (6.4/1.1 nm) film by means of argon ion milling using the PMMA as a mask layer. In this case, Au lines approximately 12 nm wide were achieved at a pitch of 35 nm. Although the pitch of the dense features is smaller than what can be obtained with PMMA positive tone, the stability of the structures is a serious problem, as can be seen from figure 4, especially when the aspect ratio (the ratio of the height to the width of the feature) is high.

Even the lines which are well developed have a tendency to occasionally be connected. The authors [26] suggested that these problems might be overcome by using a thinner resist layer, but this will make the transfer process more difficult to realize. Using PMMA in positive tone, Cumming *et al* [27] fabricated 3 nm wide NiCr wires at approximately 100 nm pitch using 100 keV EBL with a beam current of 12 pA and a 50 nm thick double layer of PMMA resist. The exposure dose was 1.8 nC cm^{-1}. They intentionally exposed lines from which several pixels had been omitted. After development (in isopropyl alcohol (IPA):MIBK in a 1:3 ratio at room temperature for 30 s), deposition of a 10 nm layer of NiCr and a lift-off process, they measured very small wires (approximately 3 nm) in the gaps of the exposed lines which are connected to wider, continuous wires (see figure 5). They believe that the wires in the unexposed area are generated by the secondary electrons (SE) from the nearby exposed regions and not by the primary electrons (PE). However, this process

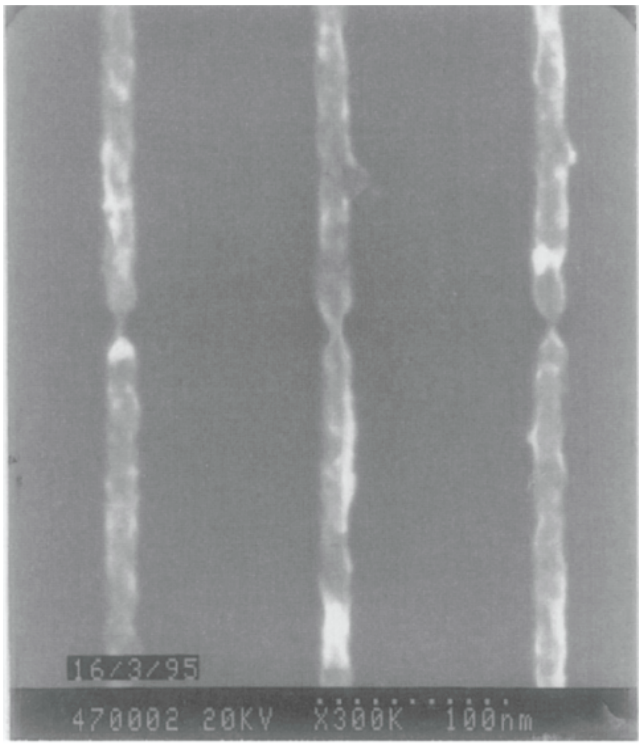

Figure 5. Approximately 3 nm wide NiCr wires using 100 keV EBL and PMMA resist [27]. Reprinted from [27]. Copyright (1996), with permission from Elsevier.

is very hard to control, because if the electron dose is too high the lines will always be continuous.

Hu *et al* [28] showed that when cold development and high electron doses are used, a higher resolution compared to the development at room temperature is obtained. This is due to the molecular weight of the PMMA which decreases when the electron dose increases, such that during cold development only the central part of the exposed region is removed by the developer, enhancing the resolution. PMMA isolated trenches of 4–8 nm at a 200 nm pitch were successfully obtained at 6 °C and by adding 1.5% methyl ethyl ketone (MEK) to the IPA developer in order to remove the PMMA residue. The initial thickness of the PMMA layer was 60 nm. Regarding dense features, linewidths of 5–7 nm were successfully patterned at a pitch of 30 nm in a 40 nm PMMA resist layer. The exposures were performed at 30 keV and with a line dose of 1.2–1.3 nC cm^{-1}. The authors also observed that, when a low temperature is used, the dissolution rate of PMMA molecules decreases, hence the loss of the PMMA molecules at the trench edges will be less than at room temperature, improving the quality of the pattern. On the other hand, a slower dissolution rate will also increase the development time, which might lead to unwanted resist etching of the isolated structures, affecting the quality of the pattern.

Several authors [29, 30] have demonstrated that by using ultrasonic development (operating frequency 38 kHz) in place of a conventional development process (usually manual immersion in a developer solution), the resolution and the resist swelling are significantly improved. In a negative tone e-beam resist, swelling always produces a broadening of the

written feature, thus swelling should be minimized. On the contrary, when swelling takes place in a positive tone e-beam resist, smaller features can be obtained but also the lithographic process is less controlled. In general, intermolecular forces and swelling of the resist are the factors which limit the resolution when using PMMA as the e-beam resist. When a resist is exposed, the intermolecular forces exerted on exposed resist molecules by unexposed molecules increase, thereby decreasing the linewidth. The exposed molecules are trapped in the potential well of the unexposed molecules and a high dose is needed in order to perform the development process. The ultrasonic development raises the potential well of the exposed molecules, favoring the development process taking place at lower doses (hence a higher resolution) and shorter development time compared with the conventional development method. Also, in this case, the solvent dissolution speed is lower due to a higher molecular weight. Therefore, the swelling of the resist (which is directly proportional to the dissolution speed) decreases when ultrasonic development is used. Moreover, for the same development time, samples developed with ultrasonic agitation need a lower dose in order to ensure the success of the development process, hence the swelling is less than for those developed conventionally. Isolated lines with 3–4 nm width and 80 nm pitch [29] were successfully obtained in a 40 nm thick PMMA resist layer, using a high-resolution e-beam patterning machine at an acceleration voltage of 80 keV and a spot size less than 4 nm. The exposure dose was 325 μC cm^{-2}. Chen *et al* [30] successfully transferred 5–7 nm wide isolated lines into the Si substrate, using reactive ion etching (RIE). The exposure conditions were similar to the ones described above, except for the thickness of the PMMA resist layer (which was about 65 nm) and the exposure dose (740 μC cm^{-2}). Still, pattern distortion and destruction of the small structures are the main disadvantages of using ultrasonic development.

Development in pure IPA [31] with ultrasonic agitation seems to work very well. With the use of pattern transfer techniques (lift-off and RIE) 20 nm lines and spaces were obtained in a 50 nm PMMA layer by using a TEM, operating in scanning mode at 200 keV. The line exposure dose was 11 nC cm^{-1}. Küpper *et al* [32] improved the PMMA resolution by using a megasonic-assisted development technique which operates at frequencies between 700 kHz and 1 MHz, reducing the risk of destroying the pattern. During ultrasonic development, microscopic gas bubbles in the developer pulse with a large amplitude, causing microstreaming of the liquid. At some point, the bubbles implode, exerting a shock wave in the developer, which can remove fragments from unexposed or exposed resist areas. However, this might also damage the pattern or even cause structures with a high aspect ratio to collapse. When the frequency increases, the size of the bubbles and their force exerted on the resist surface becomes smaller, hence the risk of destroying the pattern decreases. Also, when a resist is developed with acoustic agitation, a boundary layer is formed on top of the resist layer which separates the resist layer from the developer. The thickness of this layer (which is directly proportional to the viscosity of the developer and inversely proportional to the acoustic frequency) should be as small as possible in order to allow the development of the resist. At megasonic agitation (1 MHz), this layer is about 0.6 μm, while at a lower frequency (ultrasonic case, 40 kHz), it is about 3.8 μm. Very high aspect ratio dense holes (exposure dose 63.4 mC cm^{-2}) and lines (exposure dose 5.8 mC cm^{-2}) (see figure 6) with a pitch down to 30 nm have been successfully fabricated in a 50 nm PMMA resist layer using cold (7 °C) megasonic agitation. The exposure was performed in a high-resolution lithography tool at 100 keV.

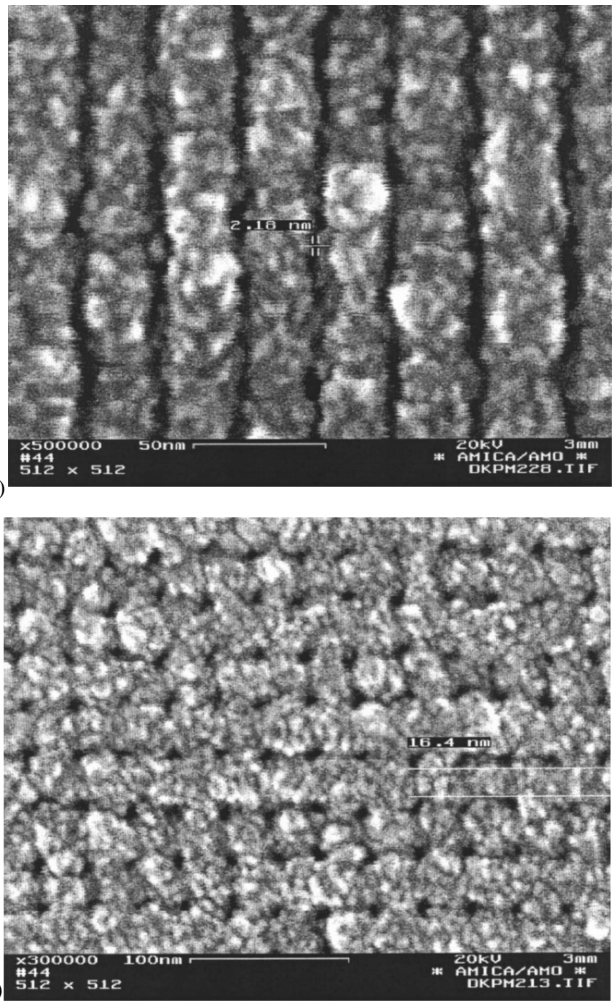

Figure 6. Sub-10-nm features written in 50 nm PMMA layer: (a) lines with 2–3 nm width, at a pitch of 30 nm; (b) nanoholes with 6 nm diameter, at a pitch of 20 nm [32]. Reprinted with permission from [32]. Copyright (2006), American Institute of Physics.

Isolated lines with a high aspect ratio (>20) have also been obtained in a 2 μm thick PMMA layer using an electron dose of 11.98 mC cm^{-2} and a development time of 50 s with megasonic agitation.

In conclusion, PMMA can be used to reproducibly obtain patterns with nm sizes. The resolution can be improved by adjusting different steps of the lithographic process such as the writing strategy or the development process. Although very small structures were successfully fabricated (<5 nm), all the written structures were isolated. Therefore, the ultimate resolution test (writing of lines and spaces) has not really been passed yet when using PMMA. Also, a frequently encountered

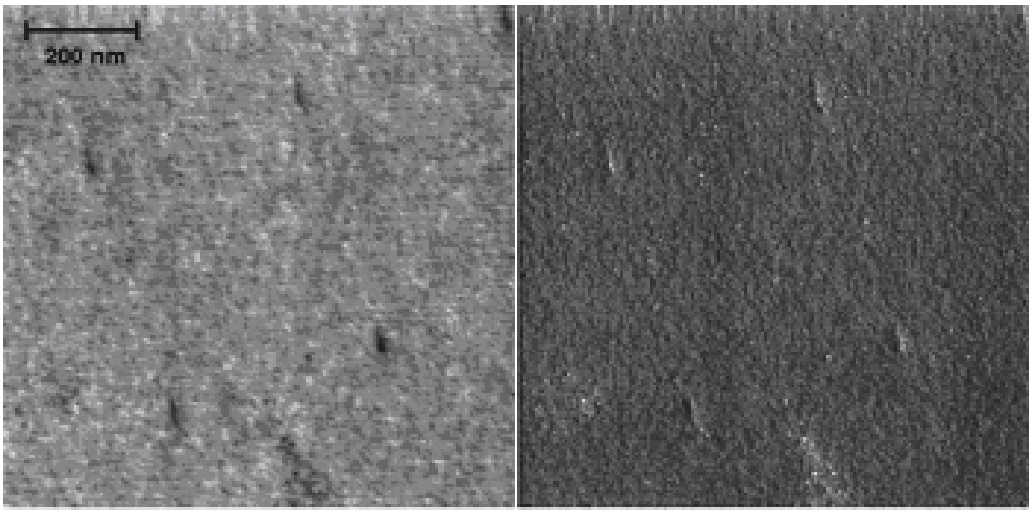

Figure 7. Atomic force microscopy (AFM, left) and friction force microscopy (FFM, right) image of approximately 5 nm dots created with the slow scan raster in a digital SEM; the exposure was performed at 20 keV, 7.6 fC/dot [40]. Reprinted with permission from [40]. Copyright (1996), American Institute of Physics.

problem of PMMA is the instability of the pattern, which tends to collapse when dense features with high aspect ratio are written.

Self-assembled monolayers (SAMs) are very good candidates for a high-resolution e-beam resist because they are homogeneous, highly ordered films of molecules with a thickness of 1–2 nm and an intermolecular spacing of 0.5–1 nm. The molecules consist of a single short organic hydrocarbon chain attached to a specific bonding group. During the self-assembly process, the bonding group attaches to the surface and the chains in the molecules order themselves due to the van der Waals interchain forces. In this way a very thin, uniform and defect-free layer is formed. Using SAMs, the contamination problem (often encountered in nanolithography) is reduced because self-assembly leads to equilibrium structures that are at (or close to) a thermodynamic minimum. Therefore SAMs tend to reject defects. In general, SAMs are prepared by exposure of the solid to vapors of reactive species or by immersion of solid substrates in solutions containing species reactive towards the surface. For example, SAMs of octadecylsiloxane were assembled on the native oxide of Si(100) wafers by immersion in dilute solutions of octadecyltrichlorosilane [OTS; $CH_3(CH_2)_{17}SiCl_3$] in hexadecane and $CHCl_3$ or CCl_4 [33]. EBL has been used to produce patterns in SAMs grown on various substrates (ranging from Si/SiO_2, Al/Al_2O_3 [34], bare GaAs and InP [35, 36] to metals (e.g. Au, Ag, Cu)) [37, 38, 34] and using different exposure tools (SEM or STM) and a beam energy ranging from 10 eV to 200 keV. Patterning of monolayers of octadecylthiol [ODT; $CH_3(CH_2)_{17}SH$] resulted in 25 nm lines and spaces (150 μC cm^{-2}) that were fabricated using a JEOL EBL system operating at 50 keV [33] and lines smaller than 15 nm (31 μC cm^{-2}) have been obtained with a STM operating at 10 eV energy [39]. The ODT monolayer was assembled on a GaAs substrate by stripping the surface oxide and then immersing the GaAs in the molten thiol. The best resolution (5 nm dots; see figure 7) was obtained in ODS (SAMs of octadecylsiloxane) layers patterned with the slow scan raster in a SEM at 20 keV [40].

In this case, the authors suggested that the resolution might be limited by the performance of the inspection tool (AFM) or by the intrinsic material limit itself. The range of the SE with enough energy to damage the material will limit the ultimate resolution if this range is larger than the molecular size. The patterns written in SAMs can be further transferred to the underlying substrate by using various etching techniques. Because SAMs are very thin, an etching process with high selectivity (which, at the same time, maintains the lateral resolution) is desired. Wet etching ensures high selectivity to the detriment of resolution, due to the isotropic etch. On the other hand, using only dry etching is not an option due to the poor selectivity. Therefore, most people used a two-step etching process, which combines wet and dry etching procedures. In the first step, a wet etch is used to define a pattern in a transfer layer (usually silicon oxide). The thickness of this layer should be as thin as possible because of the isotropic nature of the wet etch, which broadens the width of the etched feature. The second step consists of using the remaining SAM (and the patterned oxide layer) as an etch mask for silicon etching using electron cyclotron resonance (ECR) or conventional RIE.

Although very small isolated features have been obtained using SAMs, dense features of similar sizes have not yet been established. Also, the complexity of the etching process prevents SAMs from being used as an ultrahigh-resolution resist.

Chemically amplified resists (CARs) are able to produce a very high resolution with low exposure doses. Almost all CARs can be exposed below 100 mC cm^{-2}, which means high sensitivity and high throughput of the lithographic process. Moreover, they have a high resistance to plasma etching and a small molecular size (approximately 1 nm). Most of these resists are extensions of the standard poly(hydroxystyrene) polymer blocked with *t*-butylcarbonyl with a sulfonium acid

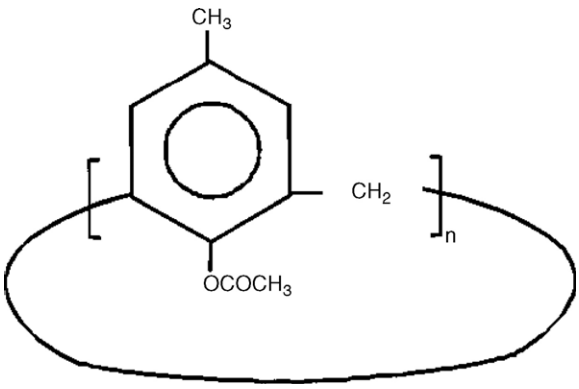

Figure 8. The chemical structure of calix[*n*] arene, where *n* is the number of phenol groups [41].

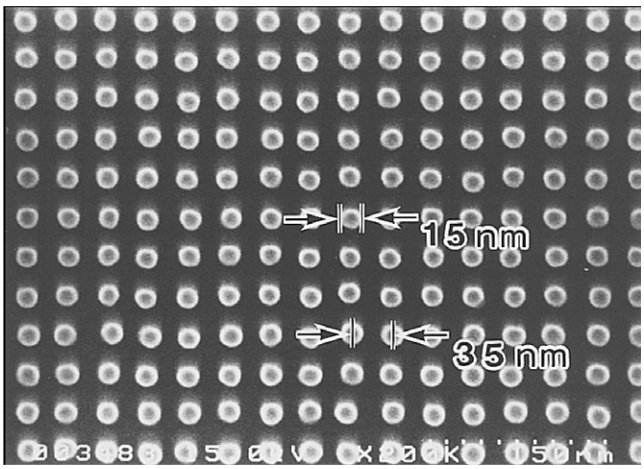

Figure 9. SEM image of 15 nm dots at a pitch of 35 nm written in 30 nm thick calixarene resist [42]. Reprinted with permission from [42]. Copyright (1996), American Institute of Physics.

generator. Rather than using exposure energy to directly cause a solubility switch, chemically amplified resists use exposure energy only to generate an acid. A typical CAR consists of a matrix copolymer and a photoacid generator (PAG). The key component in the polymer is a deprotection unit. After e-beam exposure and acid generation, a post-exposure thermal bake step is performed to catalyze the reaction between the acid molecule and the protecting group incorporated in the polymer backbone. The generated acid initiates a chain reaction or promotes a cascade of solubility-switching reactions in the exposed regions of the resist. One chemical conversion can cause several chemical reactions and thus the exposure is said to be chemically amplified. In this way, structures can be written at low exposure doses, saving time and money in the manufacturing process. There is a wide variety of chemically amplified resists with different base polymers and acid generators as primary components in the polymer matrix. One of them is calixarene which has a cyclic structure, as illustrated in figure 8 [41], and a molecular size of less than 1 nm.

Dots having 15 nm (see figure 9) diameter and 35 nm pitch (64 mC cm^{-2}) were successfully fabricated in a 30 nm calixarene resist layer on a Si substrate at 50 keV acceleration voltage [42].

The edge smoothness of the pattern is due to the molecular uniformity of the resist and its small molecular size. Sub-10-nm isolated lines (shown in figure 10) were patterned in a 20 nm resist layer using a JEOL direct e-beam writing system (JBX-5FE) operating at 50 keV and a Hitachi SEM (S-5000) operating at 30 keV [43].

Although chemically amplified resists have many advantages, they have one major disadvantage: the acid generated in the exposed area might diffuse over several nanometers into the unexposed area, causing blurring of the latent image. Kruit *et al* [44] have shown, using Monte Carlo simulations, that an increasing diffusion length of the acids in chemically amplified resists has two effects: to average the shot noise over a larger area and to decrease the resolution. Thus there is an optimum diffusion length.

Other possible candidates for high-resolution e-beam resist are fullerenes or polysubstituted derivatives of triphenylene because of their small molecular size and high dry etch durability. Depending on the exposure dose, they can be used either as positive or negative tone e-beam resists [45, 46]. The performance of polysubstituted derivatives of triphenylene (e.g. 2,3,6,7,10,11-hexapentyl-oxytriphenylene, see figure 11) demonstrated a higher dry etch durability than, for instance, the negative tone e-beam resist SAL 601, which is known for being an e-beam resist with relatively high etch resistance [46].

Isolated dots and lines with sizes of approximately 20 nm were fabricated in a 20 nm resist layer using a SEM operating at 30 keV. The exposure dose was 30 fC/dot for the dots and 60 nC cm^{-1} for the lines. Furthermore, using this resist as a mask, isolated lines with 10 nm aspect ratio have been obtained in silicon using ECR–RIE.

The difficulty of fabricating thin, uniform, defect-free resist layers and the low sensitivity seem to be the main limiting factors for these molecular resists. By adding an epoxy crosslinker (Dow DEN438) for chemical amplification and by spin coating the resist on freshly cleaved substrates, the defect density in the resist film was decreased to very low values [47]. Robinson *et al* [48] studied the effect of chemical amplification on the sensitivity of fullerene and triphenylene derivatives. The sensitivity of a MF03-04 fullerene (which is a mixture of tetra, penta and hexa methanofullerenes with hydroxyl terminated polyether add-ends) was significantly enhanced from 550 to 8 μC cm^{-2} when it was chemically amplified with a photoacid generator in combination with a crosslinker. The same behavior is observed in the case of a triphenylene with three pendant epoxy groups (C5/Epoxide) where the sensitivity is increased from 610 to 7.5 μC cm^{-2} by adding a photoacid. This high sensitivity was obtained to the detriment of the resolution. However, isolated lines down to 25 nm width were successfully patterned.

2.2. Inorganic resists

Whereas the most commonly used organic resists are polymers, inorganic resists are, in general, monomeric species. Under e-beam irradiation their chemical structure is changed, which leads to variations in the dissolution rate when the development takes place. Compared with the organic resists, the

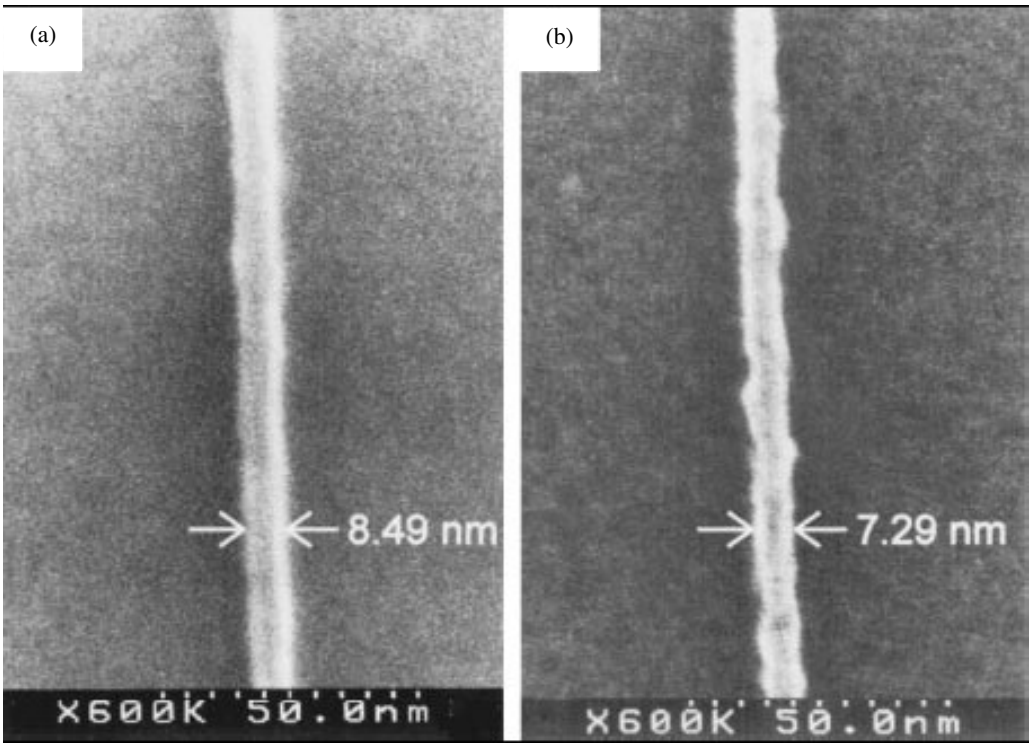

Figure 10. Sub-10-nm isolated lines obtained in 20 nm calixarene resist layer using (a) JBX-5FE and (b) S-5000 as lithographic tools [43]. Reprinted with permission from [43]. Copyright (2003), Japan Society of Applied Physics.

inorganic resists exhibit higher contrast (due to the large difference between exposed and unexposed regions) and higher etch resistance (due to their chemical structure) but lower sensitivity. They can be either vacuum deposited (e.g. metal halides) or spin coated (e.g. HSQ). Some of the ultrahigh-resolution inorganic resists are discussed below.

Metal halides such as LiF, AlF_3, $LiF(AlF_3)$ and NaCl have been studied as self-developing inorganic e-beam resists. They can be prepared by vacuum evaporation as uniform films and can also be used as a mask for RIE pattern transfer due to their high etch resistance. Most of the exposures of metal halides were performed in a scanning transmission electron microscope (STEM), using a Si_3N_4 membrane as a substrate [49]. Regarding the exposure doses, metal halides can be classified into three categories. The first one includes self-developing resists such as AlF_3, LiF and NaCl which are developed during e-beam irradiation by the dissociation of the metal halide molecules into their metal and halide components. For a complete exposure they require high electron doses in the range of 1–100 C cm^{-2}. Some of them (e.g. AlF_3) exhibit volatilization of metal fluorides in the exposed areas. Others, like LiF, will exhibit only volatilization of the fluorine component and radial diffusion of the metal component at the substrate surface, away from the exposed area. In both cases, a positive relief structure is formed *in situ* in the exposure system and no development step is required. Muray *et al* [50] observed that an exposure dose of 10 C cm^{-2} is sufficient to produce total mass loss in a 80 nm thick AlF_3 film. A dense array of very small holes of approximately 2 nm in diameter and 4 nm pitch has been successfully fabricated using a STEM at 100 keV (see figure 12).

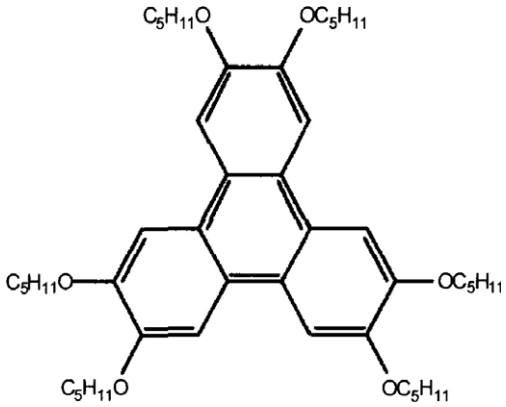

Figure 11. Representation of the 2,3,6,7,10,11-hexapentyl-oxytriphenylene molecule [46].

Fujita *et al* [51] improved the sensitivity of metal halides by using a novel technique for the deposition of AlF_3 resist films partially doped with LiF. They used a multi-target (LiF, $(Li_{0.9}Al_{0.1})F_y$ and $(Li_{0.7}Al_{0.3})F_y$) ion beam sputtering method in which the chemical composition of the film was adjusted by controlling the flux ratio from the targets having different chemical composition. The ion beam sputtering reduced the resist grain size below 10 nm even at room temperature. Five-nm lines (line dose 100 nC cm^{-1}) at a 30 nm pitch (shown in figure 13) were formed in a 10 nm resist thickness using a SEM at 30 keV with 1.5 nm beam diameter. The pattern transfer to the substrate was not very successful due to some residues which remained in the pattern after the development.

The second category includes resists (CaF_2, MgF_2) which also require relatively high exposure doses (approxi-

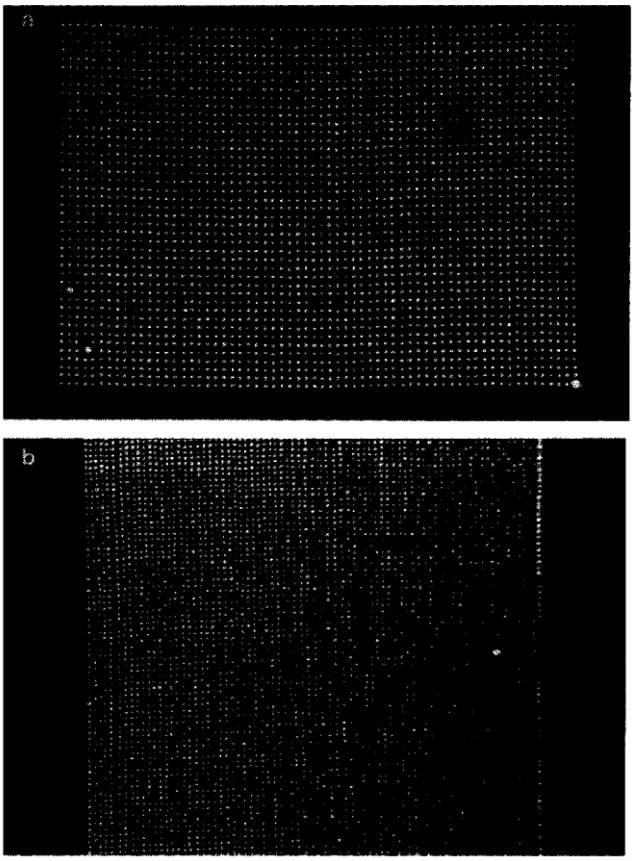

Figure 12. Annular dark field STEM image (ADF-STEM) of arrays of holes in AlF_3 resist: (a) 4 nm diameter and 8 nm pitch; (b) 2 nm diameter and 4 nm pitch [50]. Reprinted with permission from [50]. Copyright (1985), American Institute of Physics.

mately 10 C cm^{-2}) because the chemical conversion of the halide to another product has to occur before the exposure is complete. These resists have to be developed in water or another suitable agent to chemically dissolve the radiolysis-induced product. The third category includes metal halides which can act as a negative resist, depending on the receiving dose (usually not higher than 0.01 C cm^{-2}).

In conclusion, patterning at high doses, the difficulties in inorganic resist coating and the delicate handling of Si_3N_4 membranes (used as substrates in STEM) prevented their large-scale application.

Several authors have reported high-resolution patterning when using *metal oxide* (AlO_x, ZnO, TiO_x) as an e-beam negative tone resist. In general, these resists are either sputtered on a substrate using a conventional rf reactive sputtering process (e.g. AlO_x) or are spin coated colloids or naphthenates. The metal naphthenates are stable viscous liquids at room temperature and consist of cyclopentanes or cyclohexanes, methylene chains $[-(CH_2)-]$, carboxylates and metals. Under e-beam exposure, the naphthenate molecules are cross-linked, increasing the molecular weight of the resist, making it insoluble in the developer. In comparison to sputtered materials, the sensitivity seems to increase by almost a factor of 10^6 when resists are spin coated and if their structure is chemically changed [52, 53]. For example, the spin-coatable

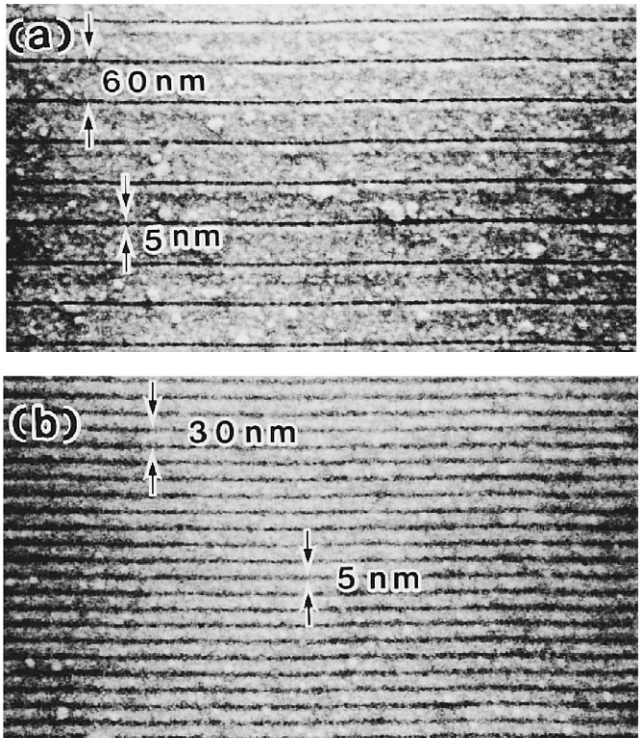

Figure 13. Approximately 5 nm wide lines written in a AlF_3-doped LiF inorganic resist at 30 keV and at two pitches: (a) 60 nm; (b) 30 nm. The line dose was 100 nC cm^{-1} [51]. Reprinted with permission from [51]. Copyright (1995), American Institute of Physics.

Al_2O_3 resists show an e-beam sensitivity of approximately 50 mC cm^{-2}, whereas for the sputtered Al_2O_3 resist the electron dose is about 5×10^6 mC cm^{-2}. In this case, we can say that the sensitivity is very similar to that when using a high-resolution organic resist such as calixarene (20 mC cm^{-2}). Compared with the sputtered metal oxide resists, under e-beam irradiation the spin coated resists seem to need only a few bonds to be broken (low dose) in order to make the irradiated area insoluble in the developer solution. Ten-nm isolated resist lines and 15 nm lines etched into silicon were obtained with a spin-coatable 60 nm thick Al_2O_3 resist layer [52]. The exposure was performed in a modified Hitachi HL-700F e-beam exposure system at 70 keV. The measured LER showed a lower value (about 2.4 nm at 300 mC cm^{-2}) than in the case of other organic resists such as ZEP 520 and SAL-601, which indicates that the aggregates have smaller sizes in the spin coated metal oxide resists. Figure 14 shows that an even higher resolution (sub-10-nm isolated and dense lines) [53] was achieved with a spin coated TiO_2 resist exposed by a high-resolution e-beam lithographic tool at 100 keV. Unfortunately, if the pitch decreases the pattern collapses, decreasing the pattern quality, as seen in figure 14(c).

Saifullah *et al* [54] fabricated 7 nm isolated lines with a high aspect ratio (approximately 10) in 100 nm ZnO–naphthenate resist using a Leica VB-6UHR nanowriter with 1.5 nm beam diameter and 2 nm beam step size. This high resolution is due to the molecular size of the resist while the strong crosslinking between the ZnO–naphthenate molecules during exposure leads to a high aspect ratio. When

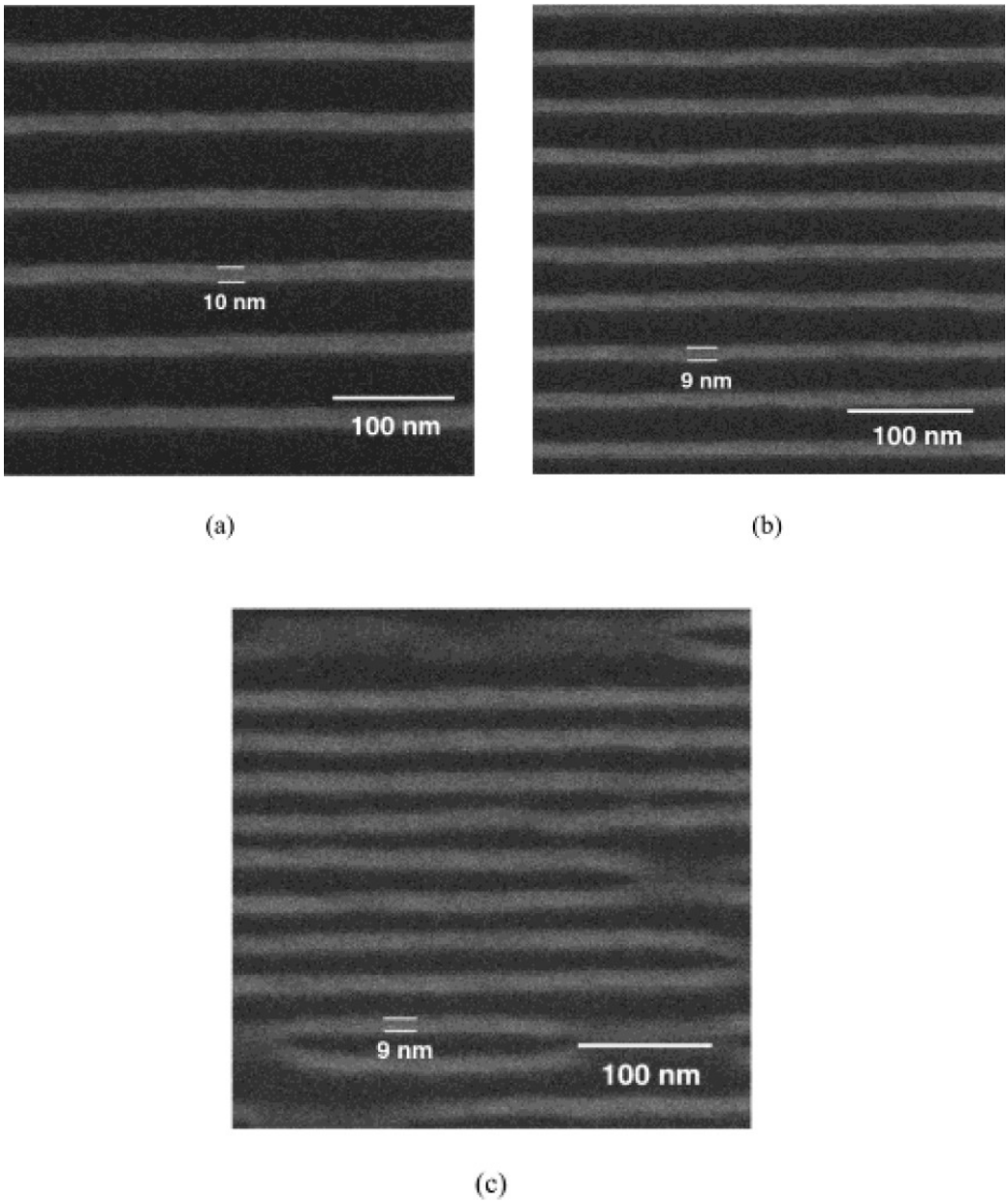

Figure 14. Sub-10-nm dense features written at a dose of 292.5 mC cm^{-2} in spin-coatable TiO_2 resist, at various pitches: (a) 60 nm, (b) 40 nm, (c) 30 nm [53]. Reprinted with permission from [53]. Copyright (2003), American Chemical Society.

samples are heated at 500 °C for an hour in air, the pattern shrinks due to the decomposition of the organic component, resulting in the appearance of crystalline ZnO. In this way, 5 nm isolated lines with low edge roughness (2.8 nm) were obtained. The improvement in the LER is caused by the uniform removal of the organic components from all sides of the lines during the heating. Although the sensitivity is relatively high (38 mC cm^{-2}), the stability of the pattern is the limiting factor when using metal oxides as high-resolution resists. For isolated nanolines with a high aspect ratio, the lines have to be supported by forming a grid in order to avoid pattern collapse. Unsupported lines require a higher dose which might decrease the resolution. Also, the dense features exhibit pattern collapse due to surface tension forces during development, blow drying or an insufficient exposure dose.

Despite their advantages (low LER, reproducibility, pattern control), instability of the pattern and the low throughput seem to be the main factors which prevent the use of spin coated metal oxide resists for nanolithographic purposes.

2.3. Nanocomposite resists

Some authors have tried to improve the properties of e-beam resists by incorporating nanoparticles (usually fullerene or silica) into the resist layer. Ishii [55] showed that the etching, mechanical and thermal resistance of the resist material are enhanced when sub-nm-size fullerene C_{60} molecules are added into the positive e-beam resist ZEP 520. These improvements are very important when writing dense nanopatterns with a

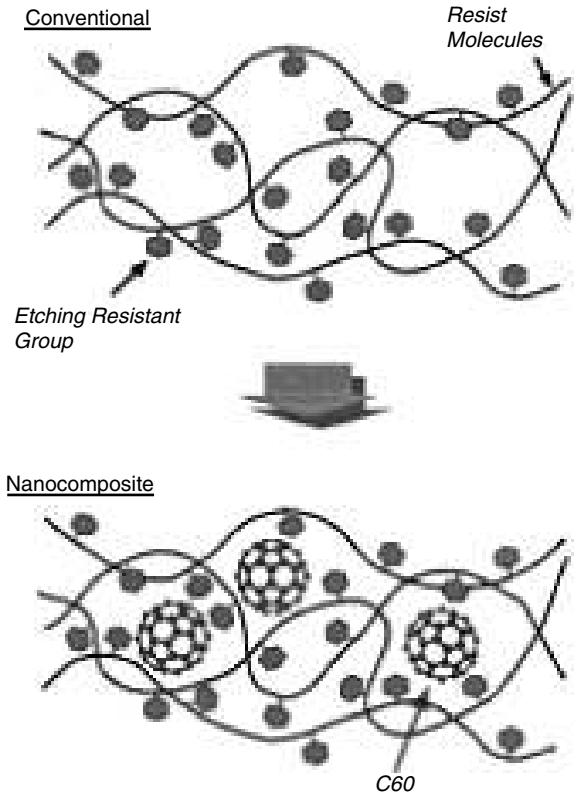

Figure 15. Concept of the nanocomposite resist system: the incorporation of sub-nm-size fullerene C_{60} molecules into a conventional resist enhances the etching resistance, thermal resistance and mechanical resistance of the resist [55]. Reprinted with permission from [55]. Copyright (1997), American Institute of Physics.

high aspect ratio because they tend to collapse due to their poor mechanical strength or etch resistance. The basic idea behind this *nanocomposite resist* system (schematically illustrated in figure 15) is that the C_{60} molecules are reducing the free volume in the spin coated resist layer, blocking the intrusion of the etching reactants in deeper regions of the resist molecules, increasing the etching resistance.

Also, because nanometer sized fullerene molecules have a high melting point (>700 °C) the thermal motion is hindered, hence the thermal resistance of the resist film is enhanced. The mechanical strength of the nanocomposite resist is enhanced because by adding C_{60} molecules the density of the film increases, therefore increasing the strength of the resist. The incorporation of 10 wt% C_{60} to the original resist solution showed enhancements of etch resistance (about 15%), thermal resistance (about 30 °C) and mechanical strength (3.5–5.5 in the aspect ratio). Exposures were performed in a 250 nm thick ZEP 520 resist layer which contains 10 wt% C_{60}, using a 25 keV Gaussian electron beam machine (JEOL-5FE). The enhancement in the etch resistance was measured with an ECR dry etch process and the improvement in the thermal and mechanical resistances was checked by imaging the pattern with the SEM. For the first, the pattern was inspected when it was heated up to 150 °C, and for the second the aspect ratios of the patterned structures were measured. The new resist system has been applied to x-ray mask fabrication and an ultrafine mask with feature sizes down to 45 nm has been successfully fabricated. Hu *et al* [56] developed a novel nanocomposite resist by adding silica particles to ZEP 520 resist which enhances the resolution and the resistance to oxygen plasma etching. When incorporating 4 wt% SiO_2 nanoparticles (relative to the bulk content of ZEP 520), an actual line of 47 nm was obtained in a 370 nm thick resist layer under 20 keV e-beam exposure. When the same experiment was performed in unmodified ZEP 520, the actual resist linewidth was 130 nm. They suggested that this improvement in the resolution is due to the silica nanoparticles (n-SiO_2 particles) which reduce the lateral spread of the SE due to a 'blocking' effect of n-SiO_2 particles. The nanoparticles have a higher atomic number than the resist material and hence a higher stopping power, which should lead to a reduction of the proximity effect in the nanocomposite resist. Although the resolution is improved, there is no significant change in the sensitivity and contrast of the nanocomposite over unmodified ZEP 520. Also, an improvement in the resolution is observed when silica nanoparticles are incorporated in a KRS-XE chemically amplified e-beam resist developed by IBM [57]. By incorporating 10.7 wt% SiO_2 nanoparticle in a KRS-XE resist layer, 100 nm lines and spaces have been successfully fabricated at 75 keV e-beam exposure. Under the same conditions, the pattern was overexposed when the unmodified KRS-XE resist was used. When the pitch is decreased to 75 nm, the features in the SiO_2/KRS-XE resist remain standing but they are not fully resolved, whereas the features in the KRS-XE resist collapse due to their high aspect ratio (greater than 4).

Although the resolution is not very good (approximately 45 nm lines and spaces), the nanocomposite resist might become suitable for nanopatterning if the process of incorporating the nanoparticles into the resist is further studied and optimized.

2.4. Overview

An overview of the best resolution (for both isolated and dense structures) and the corresponding exposure electron dose of all the discussed e-beam resists is given in table 1. Here, 'dense' stands for structures where the linewidth is equal to half the pitch ('lines and spaces') or 1/3 at minimum. Also, the main resolution-limiting factors for each type of e-beam resist are mentioned.

As we see, the smallest isolated and dense features were obtained using PMMA, and metal halides at relatively high exposure doses. Although in this case, the resolution is excellent (2–5 nm), pattern collapse and the low etch resistance prevents PMMA from being a suitable e-beam resist for nanolithography. For metal halides, the experiments were performed in a STEM, therefore the delicate handling of the Si_3N_4 membranes makes the experiments quite difficult. Also, it is not easy to find application of these small structures when they are not written on a bulk substrate. For a better visualization of the data present in table 1, we plotted the feature size (for both cases, isolated and dense structures) as function of the area dose (see figure 16). In order to have the

Table 1. Overview of the discussed e-beam resists and the smallest structures achieved with these resists.

Resist type and thickness	Smallest isolated features and exposure dose	Smallest dense features and exposure dose	Limiting factors
PMMA			
40 nm (isolated) 50 nm (dense)	5 nm wide lines at a pitch of 80 nm; dose = 325 μC cm^{-2} [29] 2–3 nm wide lines at a pitch of 30 nm; dose = 6.9 mC cm^{-2} [19]	—	Collapse of the pattern, low etch resistance
SAMs			
2 nm (isolated and dense)	5 nm dots at a pitch of 300 nm; dose per dot = 7.6 fC/dot [40]	25 nm lines and spaces; dose = 150 μC cm^{-2} [33]	Complexity of the etching process
CARs			
40 nm (isolated) 60 nm (dense)	Lines smaller than 10 nm at a pitch of 100 nm; line dose = 6.5 nC cm^{-1} [43]	15 nm dots at 35 nm pitch dose of 64 mC cm^{-2} [42]	Controlling the development process due to its complex chemical structure
Fullerene			
60 nm (isolated) 20 nm (dense)	25 nm lines at a pitch of 500 nm; dose = 200 pC cm^{-2} [48] 17 nm dots and 14 nm lines at 200 nm pitch; dose per dot = 3×10^{-14} C/dot line dose = 6 μC m^{-1} [46]	—	Difficulty of fabricating thin, defect-free film resist layers; low sensitivity
Metal halides			
20 nm (isolated) 80 nm (dense)	5 nm wide lines at a pitch of 30 nm; line dose = 100 nC cm^{-2} [51]	2 nm holes at a pitch of 4 nm; dose per hole: 10 C cm^{-2} [50]	High doses; spin coating problems
Metal oxide			
100 nm (isolated) 45 nm (dense)	7 nm wide lines at a pitch of 100 nm; dose = 38 mC cm^{-2} [53]	Sub-10-nm wide lines at a pitch of 30 nm; dose = 292.5 mC cm^{-2} [54]	Instability of the pattern; low sensitivity
Nanocomposite			
380 nm (isolated) 275 nm (dense)	47 nm wide lines at a pitch of 2 μm; dose = 25 μC cm^{-2} [56]	100 nm lines and spaces dose = 26 μC cm^{-2} [57]	Insufficient knowledge of the process of incorporating nanoparticles into the resist layer

same units (mC cm^{-2}) for each of the resists, the given line dose for some of them had to be converted to an area dose. The assumption was made that the measured linewidth (after the development process) was equal to the designed linewidth. In this case, area dose = line dose/measured linewidth.

Figure 16(a) shows that, when representing the isolated feature size versus the dose, the points are broadly scattered. On the other hand, for dense features, a virtual curve can be drawn through the values representing an inversely proportional relation between dose and feature size (see figure 16(b)). The difference between the two graphs highlights the importance of writing dense (instead of isolated) nanostructures. In this way, the risk of achieving small features due to underexposure or underdevelopment, for example, is diminished.

Another general remark is that all of the presented experiments (except for the SAMs) were performed on relatively thick (20–380 nm) resist layers. We know that by using ultrathin resist layers, the electron scattering both in the resist and in the substrate is limited, hence increasing the resolution (see figure 17). A thicker resist layer implies not only an increase in the forward scattering but also generation of more secondary electrons in the resist, which will negatively affect the resolution.

In conclusion, none of the above presented resists meets all the requirements for a successful nanolithographic process. Actually, an ideal resist material should combine the properties of an organic (high sensitivity, good reproducibility) and inorganic resist (high contrast, high resolution, high etch resistance, low LER).

Still, in the last decade, HSQ (Flowable Oxide, FOx-12 from Dow Corning) has become a serious candidate for a high-resolution e-beam resist (see figure 16(b)) because of its small line edge roughness, high etching resistance and small molecular size [22]. HSQ is also an excellent resist for testing e-beam machine resolution limits because HSQ lines on silicon can be imaged directly in a SEM without the need for gold evaporation for conduction or 'lift-off' techniques [58]. Sub-10-nm isolated and dense features have been successfully fabricated using 100 keV EBL [59–61]. Low LER (below

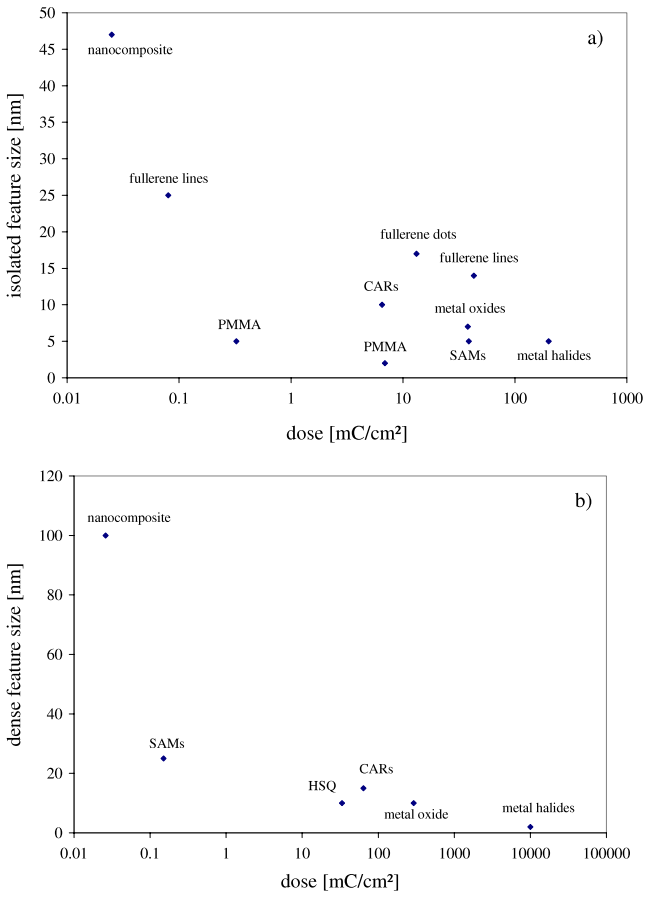

Figure 16. Feature size versus the electron dose using the data from table 1: (a) isolated features; (b) dense features.

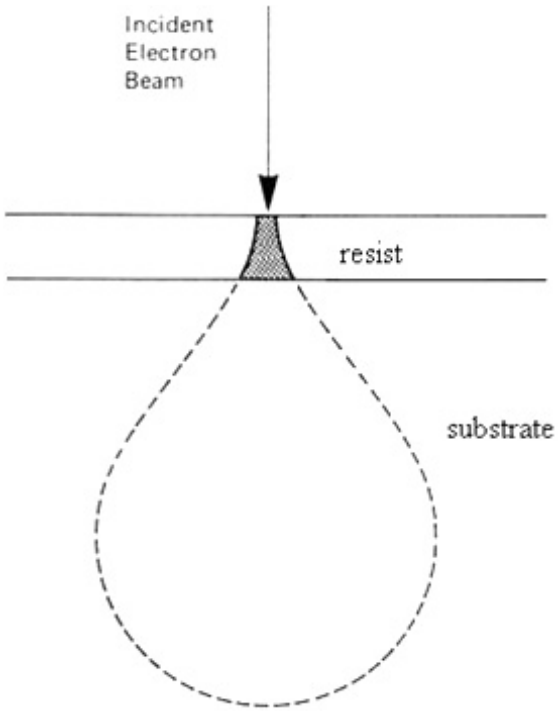

Figure 17. Schematic representation of electron scattering in resist and substrate.

2 nm) and high etch resistance (for single and bilayers) have been reported in several papers [22, 59, 62]. The properties of the resist (e.g. contrast, sensitivity, etch resistance) are influenced by numerous factors ranging from the manner of storage to the details of the development process. Therefore, in the following section we will discus all these factors step by step.

3. HSQ and electron beam lithography

3.1. Brief introduction to HSQ

Initially, the properties of the simplest member of the family of spherosiloxanes oligomers, e.g. HSQ, were studied by Frye and Collins [63]. Later on, because of its properties (low dielectric constant, ranging between 2.6 and 3, excellent gap fill and planarization performance), HSQ started to be used as an interlayer dielectric material in high-performance integrated circuits [64–66]. The use of multiple metal interconnect layers became very trivial in the semiconductor industry, due to dimension shrinkage of the devices. These multilayers are fabricated by deposition of thin silicon oxide films (by spin coating silicon-based polymer solution) which planarize the local wafer topography and enhance the formation of void-free dielectric material between adjacent metal layers. Solutions of HSQ resin have been successfully used as these planarizing oxide films. A low dielectric constant lowers the capacitance between adjacent metal interconnects, reducing electrical delay and increasing the information processing rate of the device. In 1998 Namatsu *et al* [22] discovered that HSQ can be used as a negative tone resist for EBL. They suggested that the silicon hydrogen bonds (which are weaker than SiO bonds) are broken during e-beam irradiation and converted to silanol (Si–OH) groups in the presence of absorbed moisture in the film. These silanol groups are unstable and condense to break the caged molecule to form a linear network. Usually, films were spin coated onto silicon wafers using Flowable Oxide® (FOx®), a commercially available HSQ resin solution manufactured by the Dow Corning Corporation (Midland, MI, USA), then baked and e-beam exposed in order to withstand the subsequent processing.

Regarding the structure [63], HSQ has a cage-like structure as shown in figure 18(a). In reality, the resist solution has a random structure of partially formed cages of various sizes (see figure 18(b)). These caged structures, which have the general formula $(HSiO_{3/2})_{2n}$, are opened during exposure and then form a network structure.

When deposited by spin coating techniques and annealed, the resulting film is an amorphous oxide with the formula $H_xSi_yO_z$. Van Delft [67] studied the effect of aging and storage on HSQ resist solutions (FOx-12, Dow Corning). He found that the aging of HSQ (which has a limited shelf life of about 6 months) enhances the sensitivity but decreases the contrast and resolution**.** When the FOx-12 solution is stored at 5 °C, contrast and the onset dose decrease with 0.1 y^{-1} and 7 $\mu C\,cm^{-2}\,y^{-1}$, respectively. This is due to a gradual oligo/polymerization of HSQ which broadens the molecular size distribution. HSQ is also very sensitive to contamination

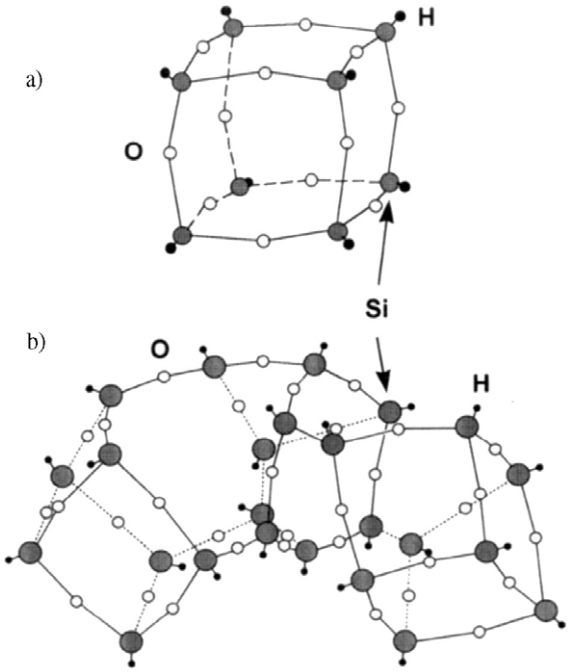

Figure 18. Schematic representation of the molecular structure of HSQ: (a) cage structure for an eight-corner oligomer; (b) random structure of the resist solution [63]. Reprinted with permission from [63]. Copyright (1970), American Chemical Society.

and therefore it should always be stored at low temperatures and in polyethylene or fluorocarbon bottles.

3.2. Spin coating of resist

When spin coating a resist on a substrate, the adhesion strength between the surfaces is determined both by the formation of chemical bonds between the surfaces and the surface roughness. If the required pattern consists of long and thin nanostructures (e.g. unsupported lines), the loss of substrate resist adhesion might become a problem. In general, in EBL, chemicals such as HMDS are widely used to improve resist adhesion to the silicon substrate. Unfortunately they are not applicable to III–V substrates or metal surfaces. One of the advantages of using HSQ is that it can be directly spin coated on Si substrates without using a primer to improve the resist adhesion to the substrate. Several authors also performed experiments on HSQ spin coated on a III–V substrate by using different tricks in order to enhance the adhesion between the resist and the substrate. For example, Macintyre *et al* [68] showed that by depositing a very thin titanium layer, the adhesion of HSQ to III–V substrates was significantly improved. They obtained 10 nm wide isolated lines written over a single 1.2 mm field using a 40 nm HSQ resist thickness and a 2 nm Ti adhesion layer. When Ti is used as an adhesion layer, the adhesion between the Ti and HSQ is promoted by the formation of Ti–O bonds between the reactive Ti and the oxygen atoms in the HSQ resist, such as Si–OH or Si–O–Si groups. Also, the authors noticed that if the HSQ is not immediately spin coated after the Ti deposition, the adhesion becomes worse due to the oxidation of Ti, which hinders the formation of bonds with the oxygen groups in the HSQ. Wi *et al* [69] enhanced the adhesion of HSQ on a Co/Pd multilayer by sputtering a 30 nm amorphous silicon (a-Si) layer on the Co/Pd multilayer. After e-beam exposure and HSQ development, the a-Si layer was used as an etch mask for transferring the pattern into the Co/Pd multilayer, increasing the etch selectivity and anisotropy. The dry etching process consisted of two steps. First, the a-Si layer was etched by a Cl_2 plasma. In the second step, the multilayer is etched by an Ar^+ plasma and the pattern is obtained. A multilayered Co/Pd nanowire array with a linewidth of 40 nm was successfully fabricated. HSQ also seems to have a good adhesion on diamond substrates, onto which dense lines with 11.5 nm width and 23 nm pitch were successfully patterned in a 35 nm resist layer [69].

Regarding the thickness of the spin coated HSQ layers, most of the experiments reported in the HSQ literature were done using 50–100 nm resist layers. Several authors [70, 60] suggested that thinner resist layers may improve the resolution that can be achieved with HSQ as a high-resolution e-beam resist. For nanolithography, where higher acceleration voltages and thinner resists are used, secondary electron generation close to the incident e-beam is expected to be the resolution-limiting factor, rather than the secondary electrons generated by the backscattered electrons [71]. In general, the main disadvantages of using ultrathin resist layers are: high defect density, lack of uniformity, inadequate etch resistance and poor contrast when nanostructures are imaged with an inspection tool. However for ultrathin HSQ layers, the last one seems to be the only drawback. Word *et al* [60] showed that very thin HSQ (25–100 nm) layers have a low roughness and are defect free, as shown in figure 19.

Grigorescu *et al* [72] reported a recipe to obtain ultrathin HSQ resist layers. By using a higher dilution rate, 1:10 FOx-12:MIBK, a 10 nm thick HSQ layer was obtained at 3000 rpm for 60 s on a Karl Suss spinner with the lid closed (in order to decrease the rate of evaporation of the solvent) (see figure 20). The HSQ spin coating was performed directly on the silicon wafer without using a primer. Sub-10-nm structures were successfully written in 20 and 10 nm thick HSQ resist layers, when using 100 keV EBL.

Clark *et al* [73] showed that the atmospheric conditions (air, nitrogen, vacuum) under which the samples are spin coated and stored influence the feature size. If the sample is spin coated in air and the same pattern is written several times with a constant dose, but after different time intervals, an increase in the feature size is observed. For example, the pattern size increases from 30 to 53 nm, if there is a time interval of 1 h between the e-beam exposures. This effect is smaller (approximately 45 nm) when the sample is prepared in nitrogen or a vacuum. When large areas are e-beam patterned, the dose should be varied in order to compensate for this exposure time delay. For example, the last written structures should have a lower electron dose than the first ones. Also, if there is a delay between the preparation of the sample and e-beam exposure, the increase in feature size is even larger, over 100%. These effects are probably due to contaminants (absorbed in the HSQ layer during waiting) which hinder network formation during the exposure. For

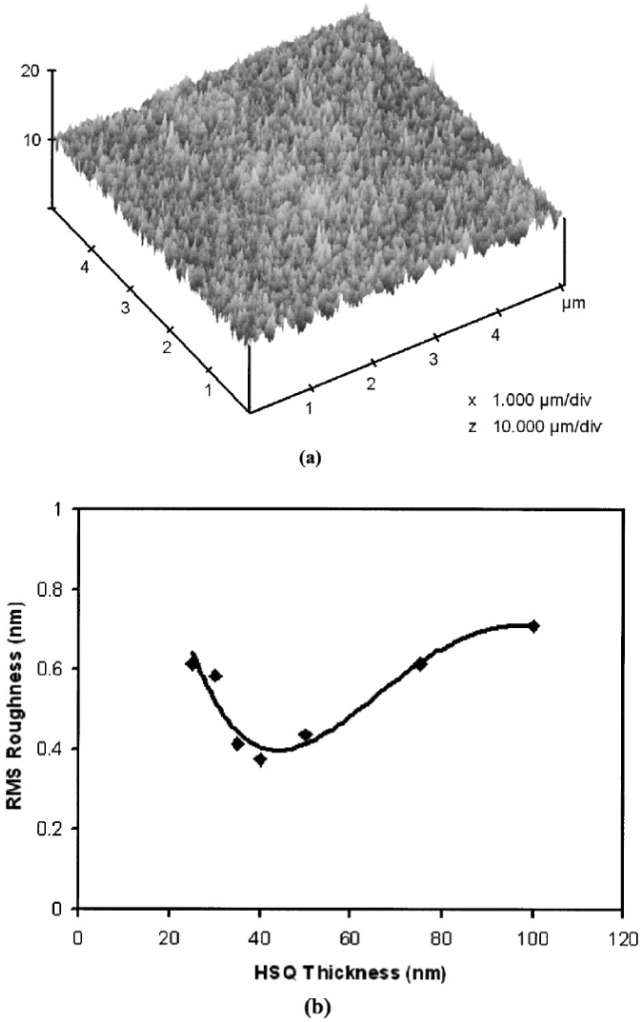

Figure 19. (a) AFM image of the surface of a 30 nm thick HSQ resist layer. (b) Surface roughness versus HSQ resist thickness [60]. Reprinted from [60]. Copyright (2007), with permission from Elsevier.

optimal results, samples should be prepared in nitrogen or a vacuum and afterward they should be exposed immediately.

Usually, the thickness and the refractive index of the spin coated HSQ layer are measured with an ellipsometer. Thickness measurements using a height profilometer, like a Tencor alphastep, on a scratch in the resist film are not easily used for HSQ due to its surface hardness.

Under thermal treatment, bond scissions and recombination occur simultaneously, favoring the transition to a network structure and reducing the cage–network ratio. The Si–H bonds are broken during baking and some of the hydrogen diffuses out. Since Si–O bonds are stronger than the Si–H bonds, the presence of oxygen during baking promotes the scission of Si–H bonds as well as the network formation. At the end of the baking process, a number of dangling Si bonds is created, due to the incomplete recombination of Si–O and Si–H bonds. For high baking temperatures, the number of dangling bonds increases but the amount of H and the cage–network ratio decreases.

Henschel and Georgiev [74, 75] studied the changes in the structure of HSQ produced by the pre-bake temperature.

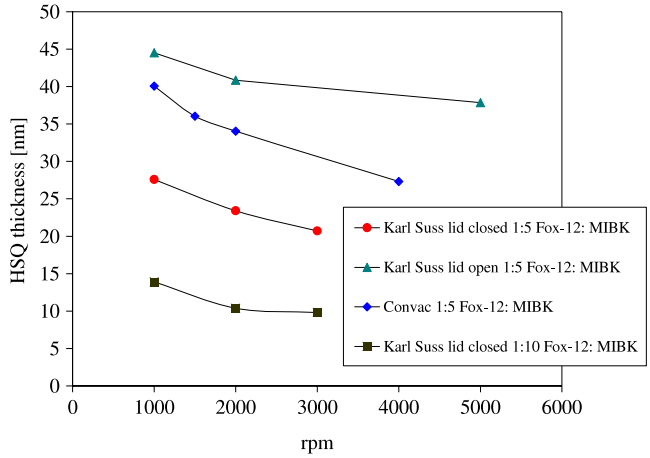

Figure 20. Spin curves for HSQ at different dilution rates and at different rotation speeds when using a Karl Suss spinner (with the lid closed or open) and a Convac spinner [72]. Reprinted with permission from [72]. Copyright (2007), Society of Photo-Optical Instrumentation Engineers.

They found that the sensitivity and roughness increase and the contrast and reproducibility decrease when high baking temperatures are used. For the surface roughness of unexposed HSQ layers baked at two different temperatures, 90 and 220 °C, they measured a value of 0.75 nm in both cases. This indicates that the influence of the baking temperature on the roughness only becomes apparent after the exposure and the development of the resist.

Van Delft [58] showed that the samples which are exposed immediately after the pre-bake exhibit higher sensitivity and lower contrast compared with the delayed ones. It was elucidated that this is due to a reversion of the network formation, the effect being more pronounced if the pre-baking temperature increases. During the pre-baking session on hot plates, a thin surface oxide layer is formed in the presence of oxygen which hinders the diffusion of oxygen into the resist layer. The thickness of this layer depends on the baking temperature, baking time and on the oxygen concentration. Henschel *et al* [74] observed that in the low temperature regime (between 90 and 120 °C), this oxidation layer has not (yet) been formed and that the network structure is slowly formed during the delay time via a slow oxidation of the Si–H or free Si bonds, leading to a lower sensitivity for delayed samples compared with the immediately exposed ones. If the samples are baked at higher temperatures (above 150 °C), the oxide layer might already have formed. In this case, only small molecules (e.g. hydrogen) can reach the resist layer and create Si–H bonds as a result of a reaction with Si dangling bonds. As a consequence, also in this case, the delayed samples have a lower sensitivity but a higher contrast compared with the ones exposed immediately.

3.3. Electron beam exposure

Direct writing EBL, based on the SEM, is the most common technique for writing very small structures in HSQ layers. Sub-10-nm lines [76, 77] have been successfully achieved when using very small spot sizes and acceleration voltages of 100 keV.

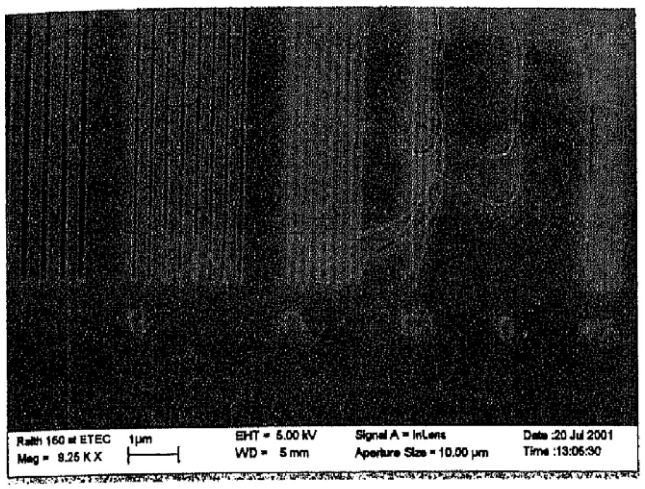

(a)

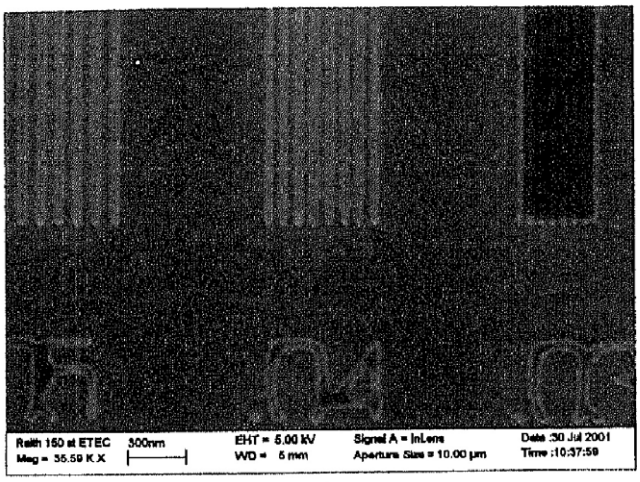

(b)

Figure 21. HSQ lines generated at 1 kV: (a) 33 nm thick resist exposed at 44 μC cm^{-2}, (b) 24 nm thick resist exposed at 40 μC cm^{-2}. Image shows 50-, 40- and 30 nm lines on a 1:1 line:space pitch [79]. Reprinted with permission from [79]. Copyright (2004), Society of Photo-Optical Instrumentation Engineers.

As we have seen in section 2, very high resolution has been obtained in inorganic resist, using a STEM [50, 78]. Despite its small beam size, the delicate handling of the sample (very small) and the use of membrane substrates impede the use of STEM as a possible exposure tool.

Several authors [79] have investigated the effect of low energy EBL on ultimate resolution. As shown in figure 21(a), the pattern is distorted due to the short penetration range of electrons in thick resist layers when low acceleration voltages are used. An improvement in the resolution is obtained when the resist thickness is decreased from 40 to 24 nm. Thirty-nm lines and spaces have been fabricated with an exposure dose of 40 μC cm^{-2} in a 24 nm HSQ layer and using an acceleration voltage of 10 keV (figure 21(b)).

Yang *et al* [80] succeeded in writing isolated lines and dots in a 50 nm thick film of HSQ (see figure 22), when using an acceleration voltage of 10 keV. The best result was 12 nm wide lines at 50 nm pitch. At 2 keV exposure energy (which implies a lower exposure dose), the minimum resolvable pitch and linewidth increase to 90 nm and 20 nm, respectively. This is due to the forward electron scattering which has a negative effect on the resolution when low energies are used. In conclusion, the authors suggested that a thinner resist layer might improve the result of the lithographic process at low energies.

There is little information regarding the writing strategy of small structures in HSQ. Grigorescu *et al* [72] suggested that when small features are desired, the ultimate resolution is set by various factors such as beam size, resist material, exposure dose, development process and also the writing strategy. Several writing strategies were discussed and an ideal recipe for obtaining small structures was presented. In general, the exposure time per pixel T (in μs) is given by $T = \frac{10DBSS^2}{I}$, where D (μC cm^{-2}) is the exposure dose, BSS(μm) is the distance between two adjacent pixel exposures (beam step size) and I (nA) is the beam current. In general there are two ways of writing structures, for example lines. Depending on the designed linewidth, an exposure is performed by scanning the beam once (single pass) over either one line (single exel or 1-exel) or n adjacent lines (n-exel line), the lines being spaced one BSS. The number of exels is defined as the number of times that the BSS fits into the designed linewidth. The method of scanning the beam more than once over a single or n-exel line is called a multiple pass line. When writing multiple passes (instead of a single pass) or an n-exel line (instead of a single exel), the dose should be lowered in order to avoid broadening of the line due to the overlap and possible proximity effects. However, in order to write the thinnest lines possible, single exel lines can be written, where the linewidth is equal to the beam size. In principle, the smaller the beam diameter that is used, the thinner the resulting line can become. However, if the beam diameter is, for example, equal to half the BSS, the line obtained after development is not continuous. When the same line is written at higher dose, the linewidth is broadened because of the proximity exposure. By doing a dose test, an optimum dose can be determined for which the linewidth after exposure and development is equal to the designed linewidth. By using n-exel single pass exposures, sub-10-nm semi-dense lines were written in a 10 nm HSQ resist layer [72] (see figure 23).

Maile *et al* [77] used a 4-exel single pass exposure at 100 keV (spotsize of 6 nm) and obtained 8 nm wide isolated lines in a 22 nm resist thickness. Van Delft *et al* [57] (see figure 24) wrote 20 nm 1:1 lines and spaces in 50 nm thick HSQ at 100 keV using single pass exposures and a BSS of 5 nm.

In all these cases, the resolution was suspected to be limited by the performance of the lithographic tool. By adjusting the electron optics of the exposure tool, 5–6 nm wide isolated lines (see figure 25) were written in a 30 nm resist HSQ layer with a spot size of 3.6 nm [76]. The exposures were again single exel single passes with a BSS of 2 nm.

Monte Carlo simulations [77] revealed that the SE are responsible for not achieving a resolution equal to the beam size. Because these electrons exit the sample surface at a distance of approximately 1 nm with respect to the point of

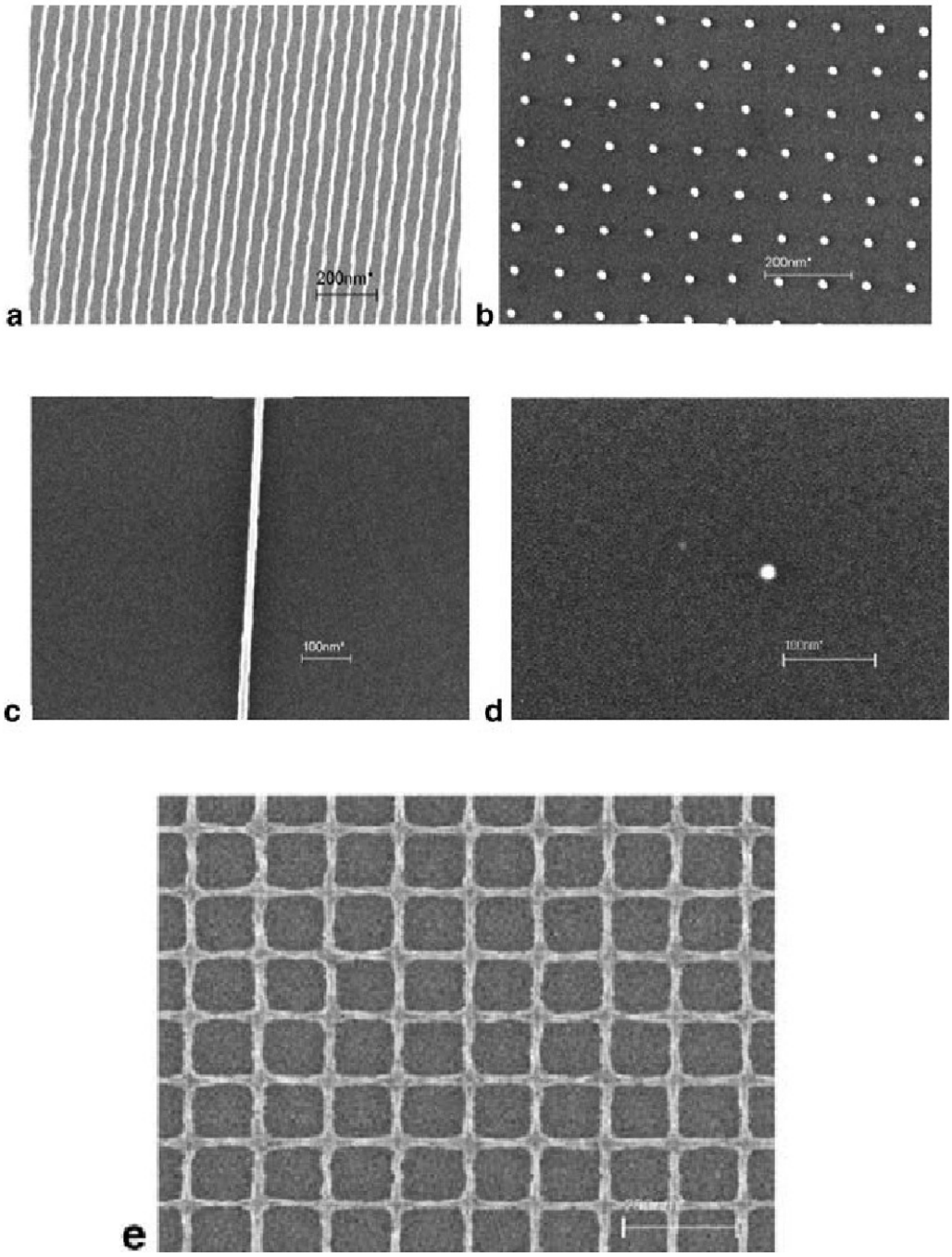

Figure 22. Lines and dots written in a 50 nm thick HSQ layer on Si at 10 keV: (a) 12 nm lines at 50 nm pitch, 420 pC cm^{-1}; (b) 15 nm dots at 100 nm pitch, 0.009 fC/dot; (c) 15 nm wide single line, 1440 pC cm^{-1}; (d) 15 nm single dot, 0.01 fC/dot; (e) mesh structure of 12 nm wide lines at 120 nm pitch, 420 pC cm^{-1} [80]. Reprinted from [80]. Copyright (2006), with permission from Elsevier.

incidence, it is assumed that a region of 0.5–1 nm on each side of the line is exposed by the SE, which explains why a 3.6 nm beam diameter cannot produce lines smaller than 5–6 nm.

In general, the main ingredients for writing small line structures are: small distance between two adjacent pixel exposures, small beam size of the exposure tool, single pass exposures.

When HSQ is e-beam irradiated, in principle the same phenomena occur as when it is pre-baked. Due to the high energy deposition, the transition to the network structure is more pronounced, leading to a lower value of the cage–network ratio and more Si dangling bonds. At low exposure doses, the cage structure dominates. If the exposure dose is increased, the formation of the network structure is accelerated and the Si bonds become more stable due to crosslinking. After the e-beam exposure, HSQ has an amorphous structure similar to SiO_2 which is relatively insoluble in alkaline hydroxide developers. Georgiev *et al* [75] observed that the roughness of the HSQ is affected by the electron dose, being more pronounced at a high baking temperature and at a low exposure dose. This is due to the local fluctuations of the network–

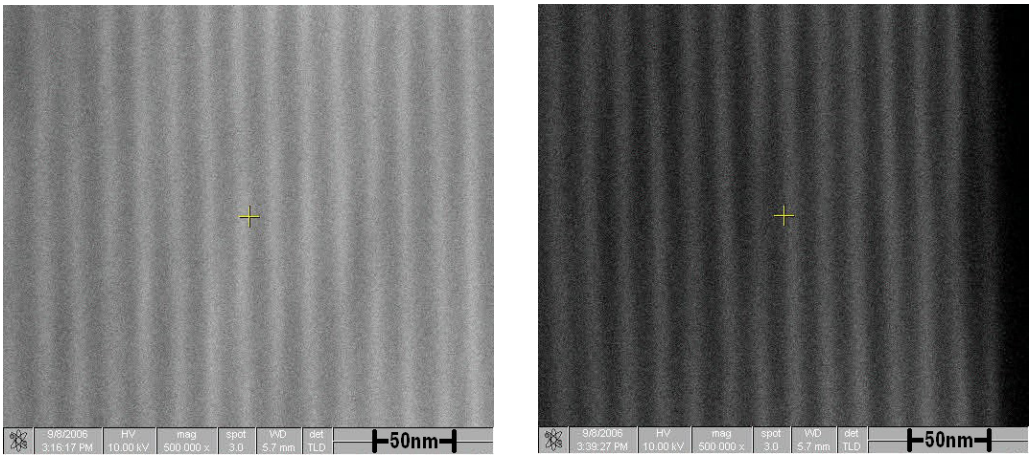

(a) (b)

Figure 23. Figure 9 SEM micrographs of *n*-exel, single pass exposures (1.25 nm beam step size, 100 keV beam energy) written in a 10 nm HSQ layer at two different area doses. The pitch is 20 nm [72]. (a) 2-exel, single pass exposure with an area dose of 70 812 μC cm^{-2} (line dose: 17.7 nC cm^{-1}); the measured linewidth is 7 nm. (b) 4-exel, single pass exposure with an area dose of 36 732 μC cm^{-2} (line dose: 18.4 nC cm^{-1}); the measured linewidth is 7.5 nm. Reprinted with permission from [72]. Copyright (2007), Society of Photo-Optical Instrumentation Engineers.

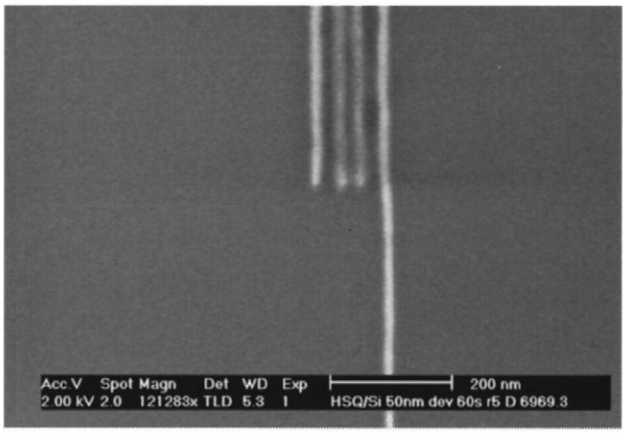

Figure 24. 20 nm 1:1 lines and spaces written in 50 nm thick HSQ at 100 kV, 7000 μC cm^{-2} [57]. Reprinted from [57]. Copyright (2002), with permission from Elsevier.

cage ratio, which prevents the development process from propagating smoothly.

The size of the structures is strongly influenced by the exposure dose. By doing a dose test, an optimum dose can be determined for a specific lithographic process at which the linewidth after exposure and development is equal to the designed linewidth. Too low or too high an electron dose leads to an under-exposed or over-exposed structure.

Van Delft [67] studied the effect of post-exposure delay time on contrast and onset dose, when samples are stored in either air or vacuum, after the e-beam exposure. He observed that both contrast and sensitivity are higher for the samples stored in vacuum in comparison to the ones stored in air, as shown in figure 26. The decrease in contrast and sensitivity after a delay time in air has been explained by a slow propagation of the network formation due to, for example, oxidation. The increase in the contrast and sensitivity, in a vacuum was not completely understood, and further investigations were suggested in order to find the answer to these effects.

Chen *et al* [81] demonstrated that a time delay of up to 4 months between the exposure and the development process does not have any influence on the lithographic properties of HSQ. Samples which were baked at 150 °C for 2 min were stored in air and the development process was performed at 18 or 20 °C. Apparently, baking at a temperature of 150 °C, followed by e-beam exposure, causes the formation of a very stable network structure of HSQ molecules. This result seems to contradict the phenomena observed by van Delft [67].

3.4. Development process

Besides the lithography tool and resist material, the development process plays an important role in the success of the e-beam patterning and this can be seen in the impressive number of papers about this process. Many experiments have been done by many workers, which proves the importance of the development time and developer concentration on the resolution. However, to reach sub-10-nm structures, a variety of extra process steps before, during or after e-beam irradiation have often been necessary. The properties of a resist material (contrast, sensitivity, process latitude) can only be obtained after the development process has been performed.

Usually, HSQ is developed by manual immersion in aqueous solutions of different developers, tetramethyl ammonium hydroxide (TMAH) being the one most frequently used [60]. Namatsu [22] suggested that the development of HSQ in alkaline solutions is related to bond scission by ionization and that the dissolution rate strongly depends on the bond strength. At low exposure doses, the dangling Si bonds are not stable and the unexposed and slightly exposed areas close to the pattern are easily dissolved even when using a weak developer. At a high exposure dose, the Si bonds become more stable due to network formation, and the dissolution rate of HSQ decreases remarkably. In this case, a strong developer

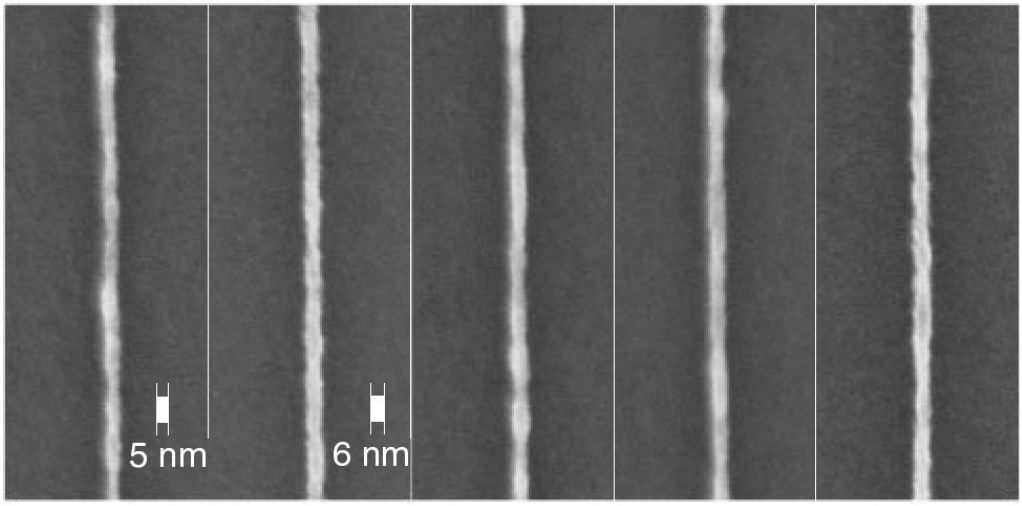

Figure 25. Six-nm wide isolated lines written with an exposure tool with a beam diameter of 3.6 nm [77]. Reprinted with permission from [76]. Copyright (2004), Japan Society of Applied Physics.

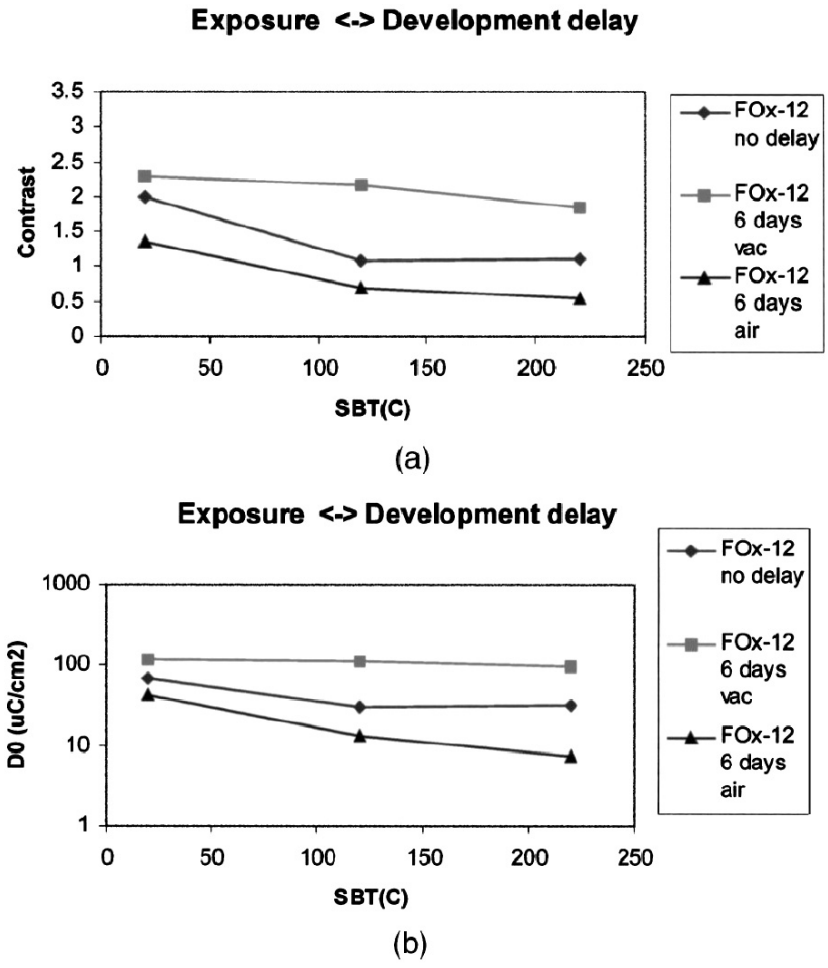

Figure 26. Effect of the post-exposure delay conditions on (a) contrast and (b) onset dose for 140 nm thick HSQ exposed at 50 kV and for different soft baking temperatures (SBT) [67]. Reprinted with permission from [67]. Copyright (2002), American Institute of Physics.

is recommended because it might improve the dissolution rate due to its effectiveness in bond scission. That means that the optimum dose shifts to higher doses, improving the contrast but decreasing the sensitivity. The main risk of using a strong developer when writing nanostructures is that the structures may be washed away and only highly exposed areas remain on the substrate. This effect has been suggested by Grigorescu *et al* [72] when writing arrays of 6 nm dots in a 20 nm

HSQ resist layer using two different concentrations of TMAH developer. MF-322 was used undiluted ($N = 0.268$ eq l^{-1}) and diluted with demineralized water in a ratio 1:3 ($N = 0.067$ eq l^{-1}). For the diluted developer, the exposed arrays of dots appeared at a lower electron dose than when the developer was undiluted. Since all samples were exposed with the same dose range, this is a clear indication that the structures that turn out to be well developed with the diluted developer are washed away in the undiluted case.

When a low developer concentration is used, the sensitivity increases but the contrast is reduced because part of the slightly exposed area near the pattern remains on the substrate.

In the search for the ultimate resolution, several other developers have been tested such as a potassium hydroxide (KOH) buffered solution (AZ 400 K from Clariant) or a sodium hydroxide (NaOH) buffered solution (Microposit 351 from Rohm and Haas) [59, 22, 75]. Grigorescu *et al* [59] studied the effect of different developers on resolution. Lines with widths between 7 and 12 nm at 20 nm pitch were successfully fabricated, and an optimum dose to define such lines was found for all developers. The main difference between the developers was found in the exposure latitude, or the slopes of the width versus dose curves. The weakest developer (MF-322) shows the steepest slopes (smallest exposure latitude) but requires the lowest dose.

The sensitivity of HSQ is increased by using non-aqueous development. Schmid *et al* [82] discovered that the dissolution of HSQ in an organic developer is rather a physical process, limited by the network formation, than a chemical process. Therefore, non-aqueous development is less aggressive towards the exposed area, leading to high sensitivity but low resolution, contrast and reproducibility. Dense lines with a pitch of 124 nm where successfully patterned at a dose of 185 μC cm^{-2} at 100 keV using xylenes as the developer for 60 s. Although the resolution is inferior compared with the one obtained with aqueous-based development, the optimization of the process can lead to better results. By using the assistance of ultrasonic agitation in the development, the thin scum between the dense lines is removed but the contrast is not significantly improved [83].

In general, the influence of the development time on resolution does not seem to be very important, especially when large structures are written in thick resist layers. The development time is usually fixed and the optimization of the development process is done by varying other parameters, e.g. baking temperature, concentration of the developer [72, 73]. When nanostructures are written in ultrathin resist layers, the development time might become an important resolution-limiting factor. If the sample is developed for too long, the structures are either washed away or etched away. In the first case, the optimum electron dose shifts to a higher value (lower sensitivity, higher contrast), leading to a broadening of the structure. In the other situation, the uncertainty in the measured linewidth increases and one way to prevent this is to write dense lines and spaces. Grigorescu *et al* [59, 72] studied the effect of the development process on the ultimate resolution of EBL using ultrathin HSQ layers. They showed that the fabrication of small structures is very complicated due to several interconnected factors which influence the final result of the e-beam patterning. In terms of ultimate resolution, they achieved 6 nm isolated dots and lines in an ultrathin HSQ layer. By refining the development process (shorter development time, a novel developer), 7 nm lines at a 20 nm pitch were written in a 10 nm thick HSQ layer, using 100 keV, 2-exel single pass, e-beam exposure at a dose of 70 812 μC cm^{-2} [72]. In the search for the ultimate resolution, they also tested different developers (MF 322, Microposit 351 and AZ 400K) with different strengths [58]. Optimum exposures could be found for lines with width between 7 and 12 nm, at a pitch of 20 nm. Lines smaller than 5 nm could not be fabricated using any of these developers, although the development time was decreased in order to prevent such small structures from being washed away from the substrate. When the development times are too short the structures may not be completely developed, leading to high sensitivity but low contrast. Dense structures (5 nm wide at a pitch of 20 nm) could be obtained using a 1:5 developer solution of Microposit 351: H_2O. Possible limits to the structure size, using HSQ, that the authors identify are the electron beam size, the resist layer thickness or the network formation process of the resist.

Usually, the development process is performed at room temperature, e.g. 21 °C. The lithographic properties of HSQ are strongly influenced by elevated development temperatures, leading to a better contrast but a lower sensitivity. Dense lines and spaces have been successfully resolved using a temperature of 40 °C, 45 °C and 50 °C respectively [82–84]. In order to have good reproducibility, one should take care that the temperature is constant during the development process.

Nowadays, when dense nanostructures with a high aspect ratio are required, pattern collapse (or distortion) becomes an important issue. For dense structures, it is possible that some of the rinsing solution (e.g. water) remains in the spaces between them. During drying, the surface tension of the rinsing solution pulls the structures towards each other, causing the pattern to collapse. For isolated features, during the development process, a fraction of the rinsing solution is absorbed in the resist. When the sample is dried, the surface of the resist dries faster than the interior. Hence, an internal stress occurs and the pattern collapses. One way to reduce the pattern collapse is to minimize the surface tension of the rinse solution by using critical point drying. With carbon dioxide (CO_2) as a supercritical (SC) drying fluid instead of the conventional resist drying under vacuum, or by nitrogen (N_2) blow, 40 nm wide lines at a pitch of 135 nm and an aspect ratio of 20 have been achieved in a 770 nm thick HSQ layer [85] (see figure 27(a)). The same method also works very well for isolated lines because the supercritical fluid can diffuse rapidly into the resist layer and remove the molecules of the rinsing solution, therefore preventing the pattern from collapsing (see figure 27(b)).

Pattern transfer to the substrate can be very challenging, especially if aspect ratios higher than 10 are desired. HSQ is an inorganic e-beam resist which has already proved its high etch resistance during the dry etching process. Trellenkamp [86] obtained 25 nm wide and 330 nm high silicon webs which

(a)

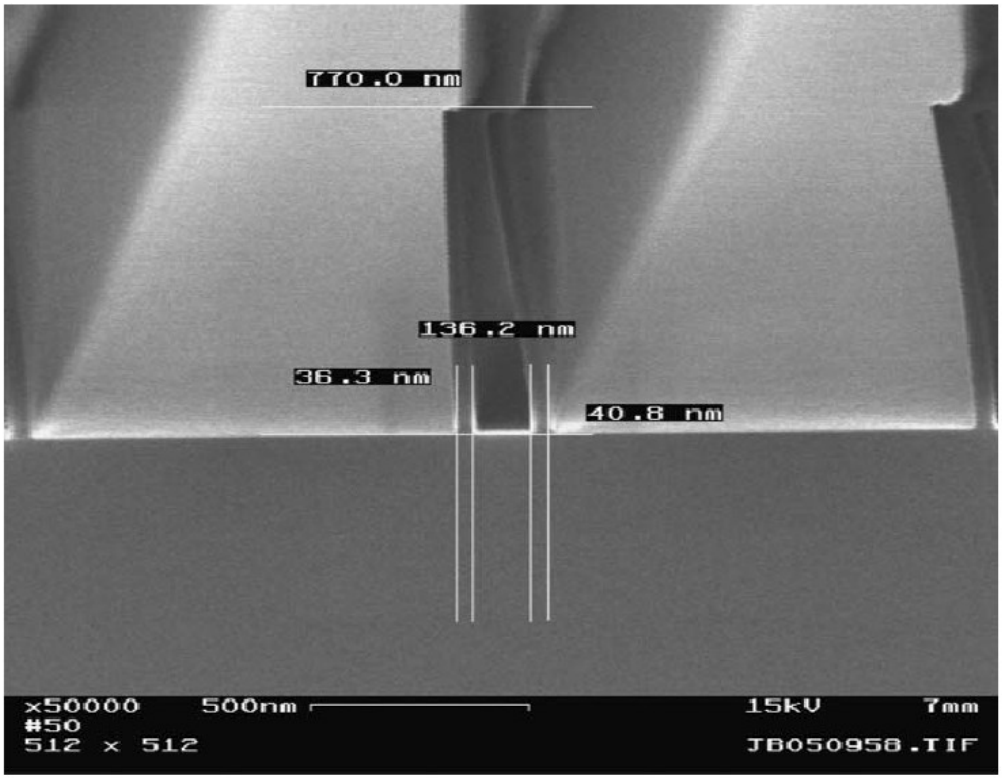

(b)

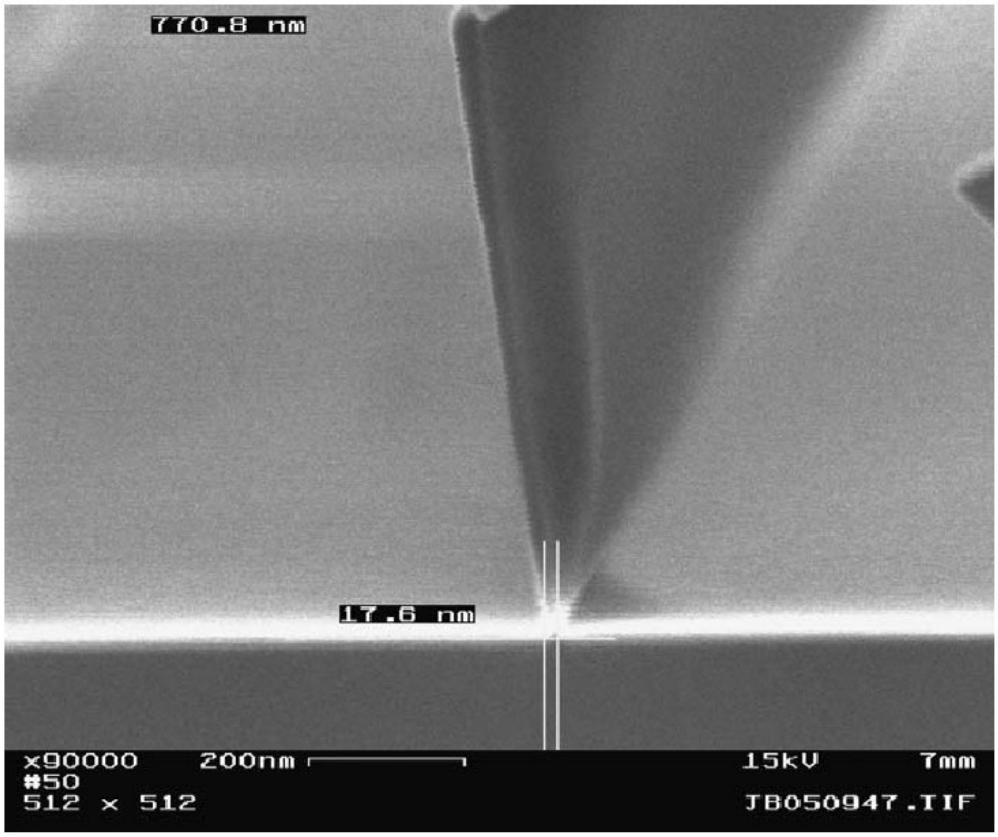

Figure 27. (a) Pair of 40 nm HSQ lines with an aspect ratio (AR) of 20, dried by SCD. (b) Isolated HSQ line with AR = 44, dried by SCD [85]. Reprinted from [85]. Copyright (2006), with permission from Elsevier.

can be used to obtain a double gate MOSFET. These structures were transferred into the silicon substrate by dry etching of a 120 nm HSQ layer with a HBr/O_2 plasma and an inductively coupled plasma (ICP) source. Twenty-nanometer lines have been successfully transferred into the silicon using HSQ as the hard mask material and an HBr/O_2 plasma [87]. The etching selectivity increases from 9.5:1 Si:HSQ to 14:1 if the resist is densified by a RTA (rapid thermal annealing) step at 1000 °C in an O_2 atmosphere. Van Delft *et al* [58] demonstrated that a very high aspect ratio can be obtained with HSQ as the top coating in a bilayer system. By using a hard baked HPR 504 film (Novolak) as the bottom layer and an O_2 RIE plasma, 300 nm wide and 3200 nm tall lines were fabricated at an exposure dose of 2000 $\mu C\,cm^{-2}$ and 50 keV acceleration voltage. They were also able to obtain 500 nm high, 50 nm wide dense lines and spaces at an exposure dose of 990 $\mu C\,cm^{-2}$ and using 50 nm thick HSQ as a mask.

Lister *et al* [70] succeeded in transfering 11.5 nm lines and spaces and isolated sub-15-nm dots into a diamond substrate, using HSQ as a hard mask and an O_2 plasma. By pre-treating the substrate with argon plasma RIE, the roughness of the transferred pattern was substantially decreased.

When a very thin resist layer is used, the resolution can be improved at the expense of low etch resistance. Yang *et al* [88] improved the etch resistance of a 50 nm HSQ layer by curing the resist after the development and prior to the RIE process. Superconducting nanowires 15 nm wide were fabricated by pattern transfer into a 6 nm thick niobium nitride (NbN) layer using CF_4 RIE and a cured HSQ resist. The etch resistance was increased by 40% by performing a second exposure step using high electron doses (between 50 and 100 $mC\,cm^{-2}$). This effect can be explained by the rapid formation of a stable network structure which increases the density of Si–O bonds and decreases the Si–H and cage Si–O bond densities.

3.5. Inspection tools

The SEM is the inspection tool most often used for imaging the result of the lithographic process. This technique is relatively easy to use and allows one to have a quick estimate of the outcome of the lithographic process. Still, when writing very small dense structures in ultrathin HSQ resist layers imaging might become an issue due to poor contrast. Since the HSQ structures consist mainly of SiO_2 there is little topographical or elemental contrast when imaged on a silicon wafer with native SiO_2 on the surface. Also, focusing becomes very difficult and the risk of pattern contamination is high. To overcome these limitations, several improvements are used, e.g. tilting the sample, lowering the acceleration voltages.

AFM is a very well established technique to characterize surface topography or morphology of individual particles. The main advantage of AFM over the traditional techniques such as SEM is that AFM directly produces three-dimensional images. The lateral size and the height of the written structures were successfully measured by AFM [82]. Also, the roughness of HSQ has been widely studied using images taken with an AFM [60, 22, 75]. The main disadvantage of AFM is that it is quite slow and the errors of measurements increase when sub-10-nm structures are inspected, because of the finite tip size.

The TEM might become, in the future, an important inspection tool. Modern TEMs have an electron probe smaller than 1 nm in diameter, in STEM imaging mode, and they allow for x-ray microanalysis and electron energy loss spectroscopy (EELS). The delicate handling of the sample (which has to be thin) is the main limiting factor in using TEM as an inspection tool. As far as we know, no HSQ experiments performed on such thin samples have been reported.

4. Applications of HSQ in lithography techniques other than EBL

Since its discovery, the number of applications of HSQ have grown continuously. In the beginning, HSQ was successfully used as a low-permittivity (low-k) interlayer dielectric in IC technology [65] and afterwards as etch mask in RIE for nanophotonic structures with low roughness [89] and imprinting masters for step and flash imprint lithography (SFIL) [90]. Also, metal oxide semiconductor field effect transistor gates with small dimension and high aspect ratio [77] have been fabricated using HSQ. In the last few years, several authors have proved that this e-beam resist can also be used with techniques [87, 91, 92] other than EBL to fabricate nanostructures. Some of these lithographic methods are described below.

4.1. Nanoimprinting

Recently, nanoimprint lithography (NIL) has started to attract a lot of attention due to its capability of creating high-resolution pattern replication with low cost and high throughput. The resist pattern is created by using a mold which physically deforms a heated polymer coated on a substrate. The mold can be made of metal or silicon dioxide deposited on a silicon substrate. After imprinting, the resist pattern is subject to RIE to produce a useful profile for the subsequent hard material pattern transfer. The resolution of the mold seems to be the most important resolution-limiting factor of NIL. HSQ started to be used successfully as a mold due to its good adhesion to the silicon substrate and because it has a structure similar to silicon dioxide, after thermal or electron beam curing. Häffner *et al* [87] presented an easy way to make a high-resolution mold by using e-beam patterning of HSQ on a silicon substrate. Lines (figure 28(a)) at a 40 nm pitch and with 18 nm width and 20 nm height were successfully patterned in HSQ. A layer of heated PMMA was further pressed with this mold resulting in reproducible imprints, as shown in figure 28(b).

In general, the molds are fabricated using EBL. Although high resolution is achieved, the throughput is low, especially when many copies of masters with large area structures are required for microfabrication. The CD, shape and aspect ratio may be affected by the etching step in the mold fabrication process. Junarsa *et al* [93] presented a novel method to fabricate molds by direct x-ray exposure of HSQ through a mask fabricated by EBL. This technique improved the CD and roughness of the patterned structures.

In a conventional NIL process, the resist undergoes a thermal cycle which can affect the accuracy of the replicated

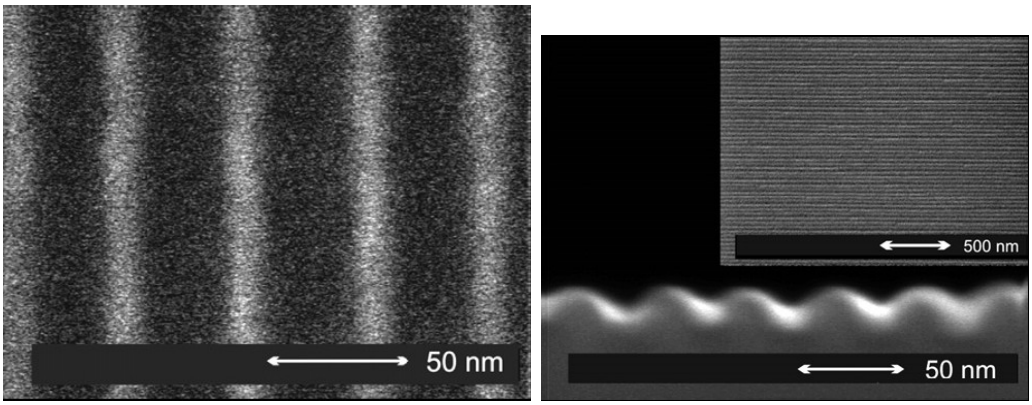

(a) (b)

Figure 28. (a) SEM image of an 18 nm wide line in HSQ at 40 nm pitch. (b) Top view and side view of imprinted lines in heated PMMA with a period of 40 nm [87]. Reprinted from [87]. Copyright (2007), with permission from Elsevier.

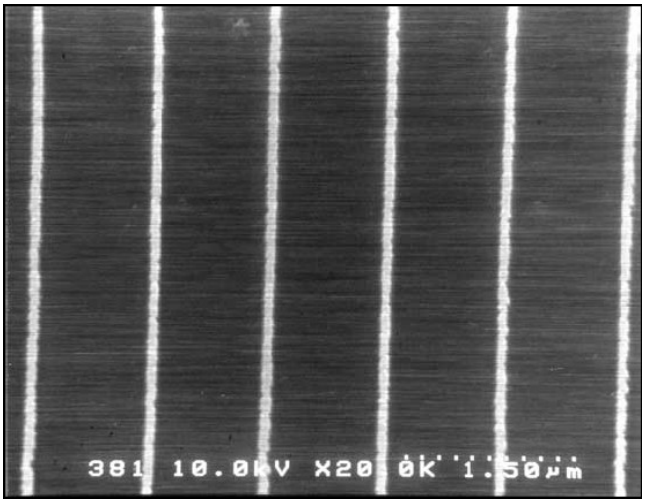

Figure 29. SEM image of 100 nm wide PdAu lines fabricated on silicon using the RT-NIL process with the PMMA/HSQ bilayer resist stack [94]. Reprinted with permission from [94]. Copyright (2003), American Institute of Physics.

pattern. In order to be deformed by a mold, the resist must first be heated above the glass transition temperature. After cooling below this temperature, the resist hardens and the mold can be released, leaving a patterned resist surface. Room temperature NIL (RT-NIL) seems to overcome these problems. Matsui *et al* [94] successfully replicated patterns with a 90 nm diameter hole and lines of 50 nm width using RT-NIL and HSQ resist instead of conventional PMMA. Other authors demonstrated that a bilayer resist process with HSQ as a top layer can be used to fabricate high aspect ratio resist patterns on a silicon substrate. Lines with 100 nm width and 1 μm height at a pitch of 200 nm were successfully fabricated in a HSQ/AZ or HSQ/PMMA bilayer resist process (figure 29).

4.2. Extreme ultraviolet (EUV) lithography

Extreme ultraviolet lithography is a technique which uses high-energy photons (with a wavelength of 13.4 nm) to pattern the resist layers. An ideal EUV resist should have high sensitivity, high contrast and high etch resistance and low LER. Several authors have studied the possibility of using HSQ as an EUV photoresist. Ekinci *et al* [92] demonstrated that HSQ has a lower sensitivity (20–25 mJ cm^{-2}) but a higher contrast (15) than PMMA (36 mJ cm^{-2}, 2.4). Twenty-nm lines at a 20 nm half-pitch have been obtained in HSQ using EUV interference lithography and high-concentration developers (TMAH, 2.6 N) and long development times (10 min). If the pre-baking temperature increases from 90 to 180 °C, the sensitivity increases but the contrast decreases, which is in agreement with the results obtained with EBL. Jurnasa *et al* [95] demonstrated that HSQ has a better sensitivity (11 mJ cm^{-2}) to EUV radiation and a lower line edge roughness (5.1 nm for 26 nm dense lines) in comparison to chemically amplified resists, making it suitable for application in EUV lithography.

4.3. Step and flash imprint lithography (SFIL)

Step and flash imprint lithography, which is a derivative of NIL, replicates patterns by a using UV transparent template having a relief image etched into its surface. To create a pattern, the wafers are first spin coated with an organic polymer transfer layer. The template, which contains the pattern, is pressed into this layer and the resist is cured upon exposure by UV irradiation. After the removal of the template, a short fluorocarbon RIE step is performed to remove the residues of the polymer layer. Finally, an oxygen etch is performed on the transfer layer and the pattern is transferred into the underlying substrate. Unlike NIL, this technique is done at room temperature and low pressures.

Mancini *et al* [90] investigated the possibility of using HSQ for direct e-beam patterning of SFIL templates. Quartz photomask substrates were coated with an indium tin oxide charge dissipation layer (ITO) and patterned with an e-beam using a 100 nm thick HSQ resist layer. Using a 60 nm transfer layer consisting of Shipley AR2 600 DUV as an etch mask, 200 mm wafers were printed with the above-mentioned template. The best resolution resulted in 25 nm lines (100 nm pitch) on templates and 40 nm lines (100 nm pitch) on imprinted wafers, as shown in figure 30.

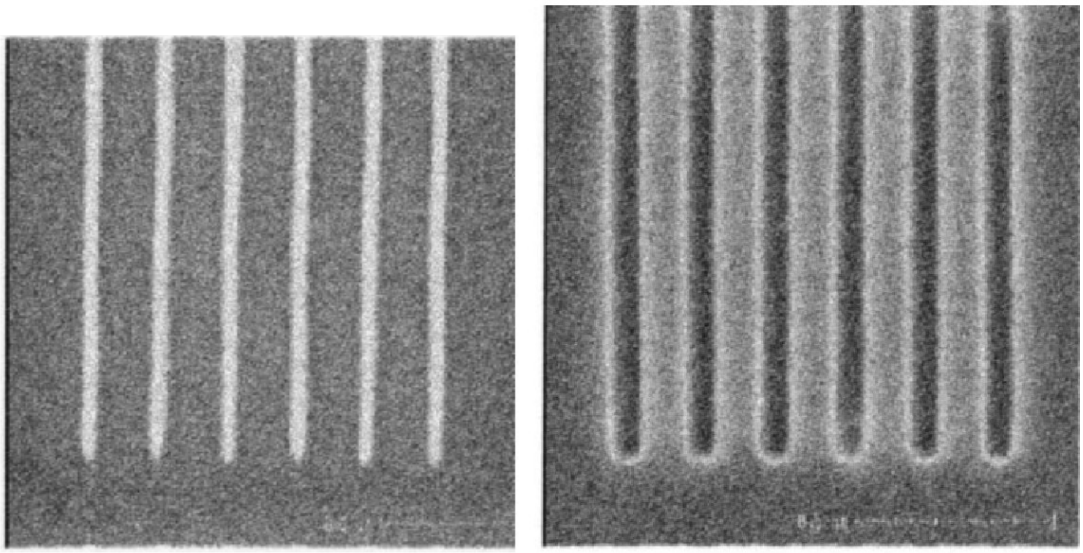

(a) (b)

Figure 30. Lines down to 25 and 100 nm pitch written with SFIL on (a) templates and (b) imprinted wafers [90]. Reprinted with permission from [90]. Copyright (2002), American Institute of Physics.

5. Conclusions and outlook

The ultimate resolution of resist-based e-beam lithography pushes the performance of both the lithographic tool and the resist material to the limit. In order to successfully write nanostructures, one should have in mind the various factors that limit the resolution, such as beam size, resist material, baking temperature, delay between baking temperature and exposure, writing strategy, exposure dose and development process. Although nowadays most of the lithographic tools have a beam diameter of a few nm (3–5 nm), it is very difficult (if not impossible) to obtain structures with sizes equal to the probe size. This limitation is due to the resist material and to different steps that the resist undergoes during the lithographic process. In the literature, there are an impressive number of papers on different materials that can be used as an e-beam resist. Unfortunately, most of these materials do not meet the requirements for being a suitable e-beam resist when sub-20-nm features are desired: high resolution and sensitivity, low LER, high etch resistance and contrast, low molecular size. Furthermore, the resist layer should be very thin (to minimize the effect of electron scattering), defect free and should have a good adhesion to the substrate The organic resists provide high sensitivity but fail in having good etch durability. Sub-10-nm isolated features can be obtained at a relatively low dose using PMMA, SAMs, CARs and fullerenes. Still, each of these resist materials has its own drawbacks (e.g. controlling the etching or the development process due to its complicated chemical structure, difficulty in obtaining very thin, defect-free resist layers) which prevent them from being widely used in lithographic processes. On the other hand, the inorganic resists are known for their small molecular size and LER and high etch resistance but also for their low sensitivity. Very dense features (2 nm holes at a pitch of 4 nm) with high aspect ratio (40) have been successfully obtained in an 80 nm thick metal halide layer using a STEM. Although the resolution is very good, the high electron dose (1 C cm^{-2}), the problems of getting uniform, defect-free layers and the delicate handling of the samples are the main difficulties encountered when using this type of resist for nanopatterning. In the ideal case, a resist material should combine the properties of organic and inorganic resists. Another thing that should be stressed here is that although very small features (<5 nm) have been successfully patterned, all of them were isolated structures (except for the metal halides). The ultimate test for EBL resolution consists of writing dense structures (see figure 16) which have the designed width equal to the half-pitch. Only then will one know for sure that the result of the lithographic process was not influenced by other factors, such as etching of the structure when a strong developer or long development time is used.

Almost 10 years ago, Namatsu suggested that a novel type of material (HSQ) could be used as an inorganic negative tone e-beam resist. Since then, more than 70 papers have reported the use of HSQ not only in EBL but also in EUV and SFIL lithography. Sub-10-nm isolated features are now frequently obtained in HSQ and even 10 nm lines and spaces have been successfully obtained with this relatively new e-beam resist. Still, the resolution is limited by factors ranging from the spin coating session to the etching process. One of the advantages of using HSQ is that very thin layers (approximately 10 nm) can be easily spun onto Si wafers, without using a primer. Also, these layers are defect free and they have a very low roughness (approximately 0.7 nm). When the resist film is pre-baked or exposed, the roughness of HSQ changes: it decreases with increasing dose and increases if a high temperature is used. In an extensive study, van Delft *et al* showed that the aging of HSQ enhances the sensitivity but deteriorates the contrast, due to a slow gradual oligo/polymerization of the resist. They also observed that a delay between the baking and exposure decreases the sensitivity but increases the contrast,

the effect being more pronounced if the baking temperature increases. Regarding the exposure, lithographic tools with a small beam diameter, operating at high acceleration voltages are recommended. In order to write very small features (e.g. lines), single exel lines should be written, where the linewidth is equal to the beam size. The sensitivity can be improved either by pre-baking the sample at high temperatures and exposing the samples immediately after the spin coating session, or by using a low-concentration developer. Sub-10-nm features have been achieved by using developers such as KOH buffered solution, or a NaOH buffered solution instead of the most frequently used TMAH. Several papers have reported an improvement in the sensitivity, when a non-aqueous developer is used (e.g. xylenes). Although the resolution is worse compared with the aqueous development (dense lines with a pitch of 124 nm), further optimization of the process might lead to better results. Ultrasonic development doesn't positively influence the resolution but it helps to remove the thin scum between the dense lines. Another parameter influencing the resolution is the development temperature, an elevated temperature leading to a better contrast but a lower sensitivity. Pattern collapse (when a high aspect ratio is desired) can be prevented by using critical point drying instead of the conventional N_2 blow, to minimize the surface tension of the rinsing solution. In this way, isolated lines with an aspect ratio of 44 have been fabricated successfully. The etch resistance of HSQ-based litho processes has been further improved either by using HSQ as a top layer in a bilayer system or by exposing the resist layer once more after the development process, but prior to the etching session.

Unfortunately, at this moment, there is no recipe which guarantees the achievement of ultimate resolution when using resist-based EBL. As we have seen, the final product of a lithographic process is determined by many factors, which are not independent of each other. For example, for HSQ (which is very sensitive to contamination) the manner of storage can already influence the resolution. Therefore, it should be always kept at low temperatures and in polyethylene or fluorocarbon bottles. Usually, one of the properties of the resist material is improved to the detriment of another. It has been demonstrated that aging, baking at low temperature, immediate exposure after spin coating, the use of a weak developer and development at a low temperature increase the sensitivity but decrease the contrast. The surface roughness is more pronounced at low exposure doses (high sensitivity) and high baking temperature. Delays between exposure and development increase both contrast and sensitivity of samples which are stored in a vacuum after the exposure, compared to those stored in air. In general, high resolution can be obtained using ultrathin resist layers and performing the exposure at high acceleration voltages. Because HSQ is a relatively new resist for nanolithography, it deserves to be further studied and analyzed. More experiments on ultrathin layers ($<$10 nm) and a better understanding of the development process (different developers with different concentrations) may very well lead to better results.

Appendix

A.1. List of symbols

Symbol	Unit	Meaning
S/N	(—)	Signal to noise ratio
D	(C m^{-2})	Exposure dose
A	(m^2)	Area of the beam spot
e	(C)	Elementary charge
D	(m)	Spot diameter
$D_{0\%}$	(C m^{-2})	Optimum electron dose
$D_{\pm 10\%}$	(C m^{-2})	Electron doses corresponding to a 10% increase or decrease in feature size
Γ	(—)	Contrast
D_2	(C m^{-2})	The minimum electron dose at which all resist thickness is lost
D_1	(C m^{-2})	The maximum electron dose at which no film thickness is lost
Σ	(m)	Parameter for characterization of line edge roughness
T	(s)	Exposure time per pixel
I	(A)	Beam current
N	(eq l^{-1})	Normality of the developer in number of mol OH^- per liter

A.2. List of abbreviations

Abbreviation	Short for
AFM	Atomic force microscope
AR	Aspect ratio
BSS	Beam step size
CAR	Chemically amplified resist
CD	Critical dimension
e-beam resist	Electron beam resist
EBID	Electron beam induced deposition
EBL	Electron beam lithography
ECR	Electron cyclotron resonance
EELS	Electron energy loss spectrometry
EUV	Extreme ultraviolet (lithography)
FFM	Friction force microscopy
HMDS	Hexamethyldisilazane primer
HPR 504	Novolak electron beam resist
HSQ	Hydrogen silsesquioxane (electron beam) resist
ICP	Inductively coupled plasma
IPA	Isopropanol
ITO	Indium tin oxide
JBX-5FE, S-5000, Hitachi HL-700F, Leica VB-6UHR, Vistec EBPG 5000+	High-resolution electron beam lithographic tools
KOH	Potassium hydroxide
KRS-XE	Chemically amplified resist
LER	Line edge roughness
MEK	Methyl ethyl ketone

MF03-04	Fullerene electron beam resist (from Cytec Cymel300)
MIBK	Methyl isobutyl ketone
NaOH	Sodium hydroxide
NIL	Nanoimprint lithography
ODS	Monolayers of octadecylsiloxane
ODT	Monolayers of octadecylthiol
OTS	Monolayers of octadecyltrichlorosilane
PAB	Post-apply-bake
PAG	Photoacid generator
PE	Primary electrons
PEB	Post-exposure-bake
PL	Process or exposure latitude
PMMA	Polymethyl methacrylate
RIE	Reactive ion etching
RMS	Root mean square
RTA	Rapid thermal annealing
RT-NIL	Room temperature nanoimprint lithography
SAL	Negative tone electron beam resist (from Shipley)
SAMs	Self-assembled monolayers
SC	Supercritical drying fluid
SCD	Supercritical drying
SE	Secondary electrons
SEM	Scanning electron microscope
SFIL	Step and flash imprint lithography
STEM	Scanning transmission electron microscope
STM	Scanning tunneling microscope
TEM	Transmission electron microscope
TMAH	Tetramethyl ammonium hydroxide
ZEP	Positive tone electron beam resist (from Nippon Zeon)

References

[1] Feynman R P 1960 There is plenty of Room at the Bottom, an invitation to enter a new field of physics *Eng. Sci. Mag.* **23** 143

[2] Newman T 1986 Tiny tale gets grand, California Institute Technol. *J. Eng. Sci.* **49** 24

[3] Einstein A 1905 A new determination of molecular dimensions *Ann. Phys.* **19** 289

[4] Knoll M 1935 Aufladepotential und sekundäremission elektronenbestrahlter körper *Z. Tech. Phys.* **16** 467

[5] Ruska E 1933 Die elektronenmikroskopische abbildung elektronenbestrahlter oberflächen *Z. Phys.* **83** 492

[6] Bacon E K 1976 *Irving Langmuir* ed W D Miles (Washington, DC: Amer. Chem. and Eng., Amer. Chem. Soc.) p 288

[7] Arthur J R Jr 1968 Interaction of Ga and As_2 molecular beams with GaAs surfaces *J. Appl. Phys.* **39** 4032

[8] Taniguchi N 1974 On the basic concept of nano-technology *Proc. Int. Conf. Prod. Eng. (Tokyo)* Japan Soc. of Precision Eng. p 245 Part II

[9] Binnig G, Rohrer H, Gerber Ch and Weibel E 1982 Surface studies by scanning tunneling microscopy *Phys. Rev. Lett.* **49** 47

[10] Kroto H W, Heath J R, O'Brien S C, Curl R F and Smalley R E 1985 C_{60}: buckminsterfullerene *Nature* **318** 162

[11] Eigler D M and Schweitzer E K 1990 Positioning single atoms with a scanning tunnelling microscope *Nature* **344** 524

[12] Iijima S 1991 Helical microtubules of graphitic carbon *Nature* **354** 56

[13] Tans S J, Verschueren A R M and Dekker C 1998 Room-temperature transistor based on a single carbon nanotube *Nature* **393** 49

[14] Yurke B, Turberfield A J, Mills A P, Simmel F C and Neumann J L 2000 A DNA-fuelled molecular machine made of DNA *Nature* **406** 605

[15] Niemeyer C M 2001 Nanoparticles, proteins, and nucleic acids: biotechnology meets materials science *Angew. Chem. Int. Edn* **40** 4128

[16] Whitesides G M 2005 Nanoscience, nanotechnology, and chemistry *Small* **1** 172

[17] Shoji H, Nakata Y, Mukai K, Sugiyama Y, Sugawara M, Yokoyama N and Ishikawa H 1997 Temperature dependent lasing characteristics of multi-stacked quantum dot lasers *Appl. Phys. Lett.* **71** 193

[18] Tang Y, Ni W X, Torres C M S and Hansson G V 1995 Fabrication and characterisation of Si–$Si_{0.7}Ge_{0.3}$ quantum dot light emitting diodes *Electron. Lett.* **31** 1385

[19] Chou S Y 1997 Patterned magnetic nanostructures and quantized magnetic disks *Proc. IEEE* **85** 652

[20] Tennant D M 1999 *Limits of conventional lithography, Nanotechnology* ed G L Timp (New York: AIP) p 164

[21] van Dorp W F, van Someren B, Hagen C W and Kruit P 2005 Approaching the resolution limit of nanometer scale electron beam indiced deposition *Nano Lett.* **5** 1303

[22] Namatsu H, Takahashi Y, Yamazaki K, Yamaguchi T, Nagase M and Kurihara K 1998 Three-dimensional siloxane resist for the formation of nanopatterns with minimum linewidth fluctuations *J. Vac. Sci. Technol.* B **16** 69

[23] Shin J, Han G, Ma Y, Moloni K and Cerrina F 2001 Resist line edge roughness and aerial image contrast *J. Vac. Sci. Technol.* B **19** 2890

[24] Yamaguchi T, Namatsu H, Nagase M, Yamazaki K and Kurihara K 1999 A new approach to reducing line-edge roughness by using a cross-linked positive-tone resist *Japan. J. Appl. Phys.* **38** 7114

[25] Haller I, Hatzakis M and Shrinivasan R 1968 High-resolution positive resists for electron-beam exposure *IBM J. Res. Develop.* **12** 251

[26] Hoole A C F, Welland M E and Broers A N 1997 Negative PMMA as a high-resolution resist—the limits and possibilities *Semicond. Sci. Technol.* **12** 1166

[27] Cumming D R S, Thoms S, Weaver J M R and Beaumont S P 1996 3 nm NiCr wires made using electron beam lithography and PMMA resist *Microelectron. Eng.* **30** 423

[28] Hu W, Sarveswaran K, Lieberman M and Bernstein G H 2004 Sub-10 nm electron beam lithography using cold development of poly-methylmethacrylate *J. Vac. Sci. Technol.* B **22** 1711

[29] Yasin S, Hasko D G and Ahmed H 2001 Fabrication of <5 nm width lines in polymethylmethacrylate resist using a water:isopropyl alcohol developer and ultrasonically-assisted development *Appl. Phys. Lett.* **78** 2760

[30] Chen W and Ahmed H 1993 Fabrication of 5–7 nm wide etched lines in silicon using 100 keV electron-beam lithography and polymethylmethacrylate resist *Appl. Phys. Lett.* **62** 1499

[31] Vieu C, Carcenac F, Pepin A, Chen Y, Mejias M, Lebib A, Manin-Ferlazzo L, Couraud L and Launois H 2000 Electron beam lithography: resolution limits and applications *Appl. Surf. Sci.* **164** 111

[32] Küpper D, Küpper D, Wahlbrink T, Bolten J, Lemme M C, Georgiev Y M and Kurz H 2006 Megasonic-assisted development of nanostructures *J. Vac. Sci. Technol.* B **24** 1827

[33] Lercel M J, Redinbo G F, Rooks M, Tiberio R C, Craighead H G, Sheen C W and Allara D L 1995 Electron

beam nanofabrication with self-assembled monolayers of alkylthiols and alkylsiloxanes *Microelectron. Eng.* **27** 43
[34] Ulman A 1991 *Introduction to Thin Organic Films: From Langmuir–Blodgett to Self-assembly* (Boston, MA: Academic) p 187
[35] Sheen C W, Shi J X, Martensson J, Parkih A N and Allara D L 1992 A new class of organized self-assembled monolayers: alkane thiols on gallium arsenide(100) *J. Am. Chem. Soc.* **114** 1514
[36] Gu Y, Lin Z, Butera R A, Smentkowski V S and Waldeck D H 1995 Preparation of self-assembled monolayers on InP *Langmuir* **11** 1849
[37] Whitesides G M and Laibinis P E 1990 Wet chemical approaches to the characterization of organic surfaces: self-assembled monolayers, wetting, and the physical-organic chemistry of the solid–liquid interface *Langmuir* **6** 87
[38] Dubois L H and Nuzzo R G 1992 Synthesis, structure, properties of model organic surfaces *Annu. Rev. Phys. Chem.* **43** 437
[39] Lercel M J, Redinbo G F, Pardo F D, Rooks M, Tiberio R C, Simpson P, Craighead H G, Sheen C W, Parikh A N and Allara D L 1994 Electron beam lithography with monolayers of alkylthiols and alkylsiloxane *J. Vac. Sci. Technol.* B **12** 3663
[40] Lercel M J, Whelan C S, Craighead H G, Seshadri K and Allara D L 1996 High-resolution silicon patterning with self-assembled monolayer resists *J. Vac. Sci. Technol.* B **14** 4085
[41] Manako S, Ochiai Y, Yamamoto H, Teshima T, Fujita J and Nomura E 2000 High-purity, ultrahigh-resolution calixarene electron-beam negative resist *J. Vac. Sci. Technol.* B **18** 3424
[42] Fujita J, Ohnishi Y, Ochinai Y, Nomura E and Matsui S 1996 Nanometer-scale resolution of calixarene negative resist in electron beam lithography *J. Vac. Sci. Technol.* B **14** 4272
[43] Ishida M, Fujita J, Ogura T, Ochiai Y, Ohshima E and Momoda J 2003 Sub-10 nm-scale lithography using p-chloromethyl-methoxy-calix[4]arene Resist *Japan. J. Appl. Phys.* **42** 3913
[44] Kruit P and Steenbrink S 2005 Local critical dimension variation from shot-noise related line edge roughness *J. Vac. Sci. Technol.* B **23** 3033
[45] Tada T and Kanayama T 1996 Nanolithography using fullerene films as an electron beam resist *Japan. J. Appl. Phys.* **35** L63
[46] Tada T, Kanayama T, Robinson A P G, Palmer R E, Allen M T, Preece J A and Harris K D M 2000 A triphenylene derivative as a novel negative/positive tone resist of 10 nm resolution *Microelectron. Eng.* **53** 425
[47] Chen X, Robinson A P G, Manickam M and Preece J A 2007 Suppression of pinhole defects in fullerene molecular electron beam resists *Microelectron. Eng.* **84** 1066
[48] Robinson A P G, Zaid H M, Gibbons F P, Manickam M, Preece J A, Brainard R, Zampini T and O'Connell K 2006 Chemically amplified molecular resists for electron beam lithography *Microelectron. Eng.* **83** 1115
[49] Kratschmer E and Isaacson M 1987 Progress in self-developing metal fluoride resists *J. Vac. Sci. Technol.* B **5** 369
[50] Muray A, Scheinfein M, Isaacson M and Adesida I 1985 Radiolysis and resolution limits of inorganic halide resists *J. Vac. Sci. Technol.* B **3** 367
[51] Fujita C, Watanabe H, Ochiai Y, Manako S, Tsai J S and Matsui S 1995 Sub-10 nm lithography and development properties of inorganic resist by scanning electron beams *J. Vac. Sci. Technol.* B **13** 2757
[52] Saifullah M S M, Kurihara K and Humphreys C J 2000 Comparative study of sputtered and spin-coatable aluminum oxide electron beam resists *J. Vac. Sci. Technol.* B **18** 2737
[53] Saifullah M S M, Subramanian K R V, Tapley E, Kang D J, Welland M E and Butler M 2003 Sub-10 nm electron beam nanolithography using spin-coatable TiO_2 resists *Nano Lett.* **3** 1587
[54] Saifullah M S M, Subramanian K R V, Anderson D, Kang D J, Huck W T S, Jones G A C and Welland M E 2006 Sub-10 nm high aspect ratio patterning of ZnO in a 500 μm main field *J. Vac. Sci. Technol.* B **24** 1215
[55] Ishii T, Nozawa H, Tamamura T and Ozawa A 1997 C_{60}-incorporated nanocomposite resist system for practical nanometer pattern fabrication *J. Vac. Sci. Technol.* B **15** 2570
[56] Hu Y, Wu H, Gonsalves K and Merhari L 2001 Nanocomposite resists for electron beam nanolithography *Microelectron. Eng.* **56** 289
[57] Merhari L, Gonsalves K E, Hu Y, He W, Huang W S, Angelopoulos M, Bruenger W H, Dzionk C and Torkler M 2002 Nanocomposite resist systems for next generation lithography *Microelectron. Eng.* **63** 391
[58] van Delft F C M J M, Weterings J P, van Langen-Suurling A K and Romijn H 2000 Hydrogen silsesquioxane/novolak bilayer resist for high aspect ratio nanoscale electron-beam lithography *J. Vac. Sci. Technol.* B **18** 3419
[59] Grigorescu A E, van der Krogt M C, Hagen C W and Kruit P 2007 Influence of the development process on ultimate resolution electron beam lithography, using ultrathin hydrogen silsesquioxane resist layers *J. Vac. Sci. Technol.* B **25** 1998
[60] Grigorescu A E, van der Krogt M C, Hagen C W and Kruit P 2007 10 nm lines and spaces written in HSQ, using electron beam lithography *Microelectron. Eng.* **84** 822
[61] Word M J, Adesida I and Berger P R 2003 Nanometer-period gratings in hydrogen silsesquioxane fabricated by electron beam lithography *J. Vac. Sci. Technol.* B **21** L12
[62] Namatsu H, Yamaguchi T, Nagase M, Yamazaki K and Kurihara K 1998 Nano-patterning of a hydrogen silsesquioxane resist with reduced linewidth fluctuations *Microelectron. Eng.* **41/42** 331
[63] Frye C L and Collins W T 1970 Oligomeric silsesquioxanes, $(HSiO_3/2)_n$ *J. Am. Chem. Soc.* **92** 5586
[64] Loboda M J, Grove C M and Schneider R F 1998 Properties of a-SiO_x:H thin film deposited from hydrogen silsesquioxane resins *J. Electrochem. Soc.* **145** 2861
[65] Liu P T, Chang T C, Tsai T M, Lin Z W and Chen C W 2003 Dielectric characteristics of low-permittivity silicate using electron beam direct patterning for intermetal dielectric applications *Appl. Phys. Lett.* **83** 4226
[66] Albrecht M G and Blanchette C 1998 Materials issues with thin film hydrogen silsesquioxane low K dielectrics *J. Electrochem. Soc.* **145** 4019
[67] van Delft F C M J M 2002 Delay-time and aging effects on contrast and sensitivity of hydrogen silsesquioxane *J. Vac. Sci. Technol.* B **20** 2932
[68] Macintyre D S, Young I, Glidle A, Cao X, Weaver J M R and Thoms S 2006 High resolution e-beam lithography using a thin titanium layer to promote resist adhesion *Microelectron. Eng.* **83** 1128
[69] Wi J S, Lee T Y, Jin K B, Hong D H, Shin K H and Kim K B 2006 Electron-beam lithography of Co/Pd multilayer with hydrogen silsesquioxane and amorphous Si intermediate layer *J. Vac. Sci. Technol.* B **24** 2616
[70] Lister K A, Casey B G, Dobson P S, Thoms S, Macintyre D S, Wilkinson C D W and Weaver J M R 2004 Pattern transfer of a 23 nm-period grating and sub-15 nm dots into CVD diamond *Microelectron. Eng.* **73** 319
[71] Hagen C W, Silvis-Cividjian N and Kruit P 2006 Resolution limit for electron beam-induced deposition on thick substrates *Scanning* **28** 204

[72] Grigorescu A E, van der Krogt M C and Hagen C W 2007 Limiting factors for electron beam lithography when using ultra-thin hydrogen silsesquioxane layers *J. Micro/Nanolithogr. MEMS, MOEMS* **6** 043006
[73] Clark N, Vanderslice A, Grove R III and Krchnavek R R 2006 Resolution limit for electron beam-induced deposition on thick substrates *J. Vac. Sci. Technol.* B **24** 3073
[74] Henschel W, Georgiev Y M and Kurz H 2003 Study of a high contrast process for hydrogen silsesquioxane as a negative tone electron beam resist *J. Vac. Sci. Technol.* B **21** 2018
[75] Georgiev Y M, Henschel W, Fuchs A and Kurz H 2005 Surface roughness of hydrogen silsesquioxane as a negative tone electron beam resist *Vacuum* **77** 117
[76] Yamazaki K and Namatsu H 2004 5 nm-order electron-beam lithography for nanodevice fabrication *Japan. J. Appl. Phys.* **43** 3767
[77] Maile B E, Henschel W, Kurz H, Rienks B, Polman R and Kaars P 2000 Sub-10 nm linewidth and overlay performance achieved with a fine-tuned EBPG-5000TFE electron beam lithography system *Japan. J. Appl. Phys.* **39** 6836
[78] Langheinrich W, Vescan A, Spangenberg B and Beneking H 1992 Homogeneous lithium fluoride films as a high resolution electron beam resist *Microelectron. Eng.* **17** 287
[79] Jamieson A, Willson C G, Hsu Y and Brodie A D 2004 Low-voltage electron beam lithography resist process: top surface imaging and hydrogen silsesquioxane bilayer *J. Micro/Nanolithogr. MEMS, MOEMS* **3** 442
[80] Yang H, Jin A, Luo Q, Gu C, Cui Z and Chen Y 2006 Low-energy electron-beam lithography of hydrogen silsesquioxane *Microelectron. Eng.* **83** 788
[81] Chen Y, Yang H and Cui Z 2006 Effects of developing conditions on the contrast and sensitivity of hydrogen silsesquioxane *Microelectron. Eng.* **83** 1119
[82] Schmid G M, Carpenter L E II and Liddle J A 2004 Nonaqueous development of silsesquioxane electron beam resist *J. Vac. Sci. Technol.* B **22** 3497
[83] Häffner M, Haug A, Heeren A, Fleischer M, Peisert H, Chaasse T and Kern D P 2007 Influence of temperature on HSQ electron-beam lithography *J. Vac. Sci. Technol.* B **25** 2045
[84] Choi S, Jin N, Kumar V, Shannon M and Adesida I 2007 Effects of developer temperature on electron-beam-exposed hydrogen silsesquioxane resist for ultra-dense silicon nanowire fabrication *J. Vac. Sci. Technol.* B **25** 2085
[85] Wahlbrink T, Küpper D, Georgiev Y M, Bolten J, Möller M, Küpper D, Lemme M C and Kurz H 2006 Supercritical drying process for high-aspect ratio HSQ nano-structures *Microelectron. Eng.* **83** 1124
[86] Trellenkamp S, Moers J, van der Hart A, Kordos P and Luth H 2003 Patterning of 25 nm-wide silicon webs with an aspect ratio of 13 *Microelectron. Eng.* **67/68** 376
[87] Häffner M, Heeren A, Fleischer M, Kern D P, Schmidt G and Molenkamp L W 2007 Simple high resolution nanoimprint-lithography *Microelectron. Eng.* **84** 937
[88] Yang J K W, Anant V and Berggren K K 2006 Enhancing etch resistance of hydrogen silsesquioxane via postdevelop electron curing *J. Vac. Sci. Technol.* B **24** 3157
[89] Lauvernier D, Garidel S, Legrand C and Vilcot J P 2005 Realization of sub-micron patterns on GaAs using a HSQ etching mask *Microelectron. Eng.* **77** 210
[90] Mancini D P, Gehoski K A, Ainley E, Nordquist K J, Resnick D J, Bailey T C, Sreenivasan S V, Ekerdt J G and Willson C G 2002 Hydrogen silsesquioxane for direct electron-beam patterning of step and flash imprint lithography templates *J. Vac. Sci. Technol.* B **20** 2896
[91] Tao J, Chen Y, Zhao X, Malik A and Cui Z 2005 Room temperature nanoimprint lithography using a bilayer of HSQ/PMMA resist stack *Microelectron. Eng.* **78/79** 665
[92] Ekinci Y, Solak H H, Padeste C, Gobrecht J, Stoykovich M P and Nealey P F 2007 20 nm line/space patterns in HSQ fabricated by EUV interference lithography *Microelectron. Eng.* **84** 700
[93] Jurnasa I and Nealey P F 2004 Fabrication of masters for nanoimprint, step and flash, and soft lithography using hydrogen silsesquioxane and x-ray lithography *J. Vac. Sci. Technol.* **22** 2685
[94] Matsui S, Igaku Y, Ishigaki H, Fujita J, Ishida M, Ochiai Y, Namatsu H and Komuro M 2003 Room-temperature nanoimprint and nanotransfer printing using hydrogen silsesquioxane *J. Vac. Sci. Technol.* B **21** 688
[95] Jurnasa I, Stoykovich M P, Nealey P, Ma Y, Cerrina F and Solak H H 2005 Hydrogen silsesquioxane as a high resolution negative-tone resist for extreme ultraviolet lithography *J. Vac. Sci. Technol.* B **23** 138